Published OnlineFirst February 23, 2011; DOI:10.1158/1078-0432.CCR-10-2008

Published OnlineFirst February 23, 2011; DOI:10.1158/1078-0432.CCR-10-2008

Enhanced Safety Profiles of the Telomerase-Specific Replication-Competent Adenovirus by Incorporation of Normal Cell-Specific microRNA-Targeted Sequences

Kumiko Sugio[1,3], Fuminori Sakurai[1,3], Kazufumi Katayama[1], Katsuhisa Tashiro[3], Hayato Matsui[1,3], Kenji Kawabata[2,3], Atsushi Kawase[4], Masahiro Iwaki[4], Takao Hayakawa[5], Toshiyoshi Fujiwara[6], and Hiroyuki Mizuguchi[1,3]

Abstract

Purpose: Oncolytic adenoviruses (Ad) have been actively pursued as potential agents for cancer treatment. Among the various types of oncolytic Ads, the telomerase-specific replication-competent Ad (TRAD), which possesses an *E1* gene expression cassette driven by the human telomerase reverse transcriptase promoter, has shown promising results in human clinical trials; however, the *E1* gene is also slightly expressed in normal cells, leading to replication of TRAD and cellular toxicity in normal cells.

Experimental Design: To overcome this problem, we utilized a microRNA (miRNA)-regulated gene expression system. Four copies of complementary sequences for miR-143, -145, -199a, or let-7a, which have been reported to be exclusively downregulated in tumor cells, were incorporated into the 3′-untranslated region of the *E1* gene expression cassette.

Results: Among the TRAD variants (herein called TRADs) constructed, TRADs containing the sequences complementary to miR-143, -145, or -199a showed efficient oncolytic activity comparable to the parental TRAD in the tumor cells. On the other hand, replication of the TRADs containing the miRNA complementary sequences was at most 1,000-fold suppressed in the normal cells, including primary normal cells. In addition, to suppress the replication of the TRADs in hepatocytes as well as other normal cells, we constructed a TRAD containing 2 distinct complementary sequences for miR-199a and liver-specific miR-122a (TRAD-122a/199aT). TRAD-122a/199aT exhibited more than 10-fold reduction in viral replication in all the normal cells examined, including primary hepatocytes.

Conclusions: This study showed that oncolytic Ads containing the sequences complementary to normal cell-specific miRNAs showed significantly improved safety profiles without altering tumor cell lysis activity. *Clin Cancer Res; 17(9); 2807–18. ©2011 AACR.*

Introduction

Oncolytic adenoviruses (Ad) are genetically engineered Ads which can kill tumor cells by tumor cell-specific replication (1, 2). Several clinical trials using oncolytic Ads have been carried out, and promising results have been reported (3–5). Various types of oncolytic Ads have been developed, and can be mainly classified into 2 groups. One type of oncolytic Ads show tumor-selective replication via deletion of certain genes, such as the *E1B-55K* gene, which are dispensable for the replication of Ads in tumor cells. The other type of oncolytic Ads possess an *E1* gene expression cassette driven by tumor-specific promoters. Various types of tumor-specific promoters are used in oncolytic Ads, including the α-fetoprotein promoter (6), prostate-specific antigen promoter (7), osteocalcin promoters (8), and cyclooxygenase-2 promoter (9).

Among these oncolytic Ads possessing tumor-specific promoters, the telomerase-specific replication-competent

Authors' Affiliations: Departments of [1]Biochemistry and Molecular Biology and [2]Biomedical Innovation, Graduate School of Pharmaceutical Sciences, Osaka University; [4]Laboratory of Gene Transfer and Regulation, National Institute of Biomedical Innovation; [4]Department of Pharmacy, School of Pharmacy, [5]Pharmaceutical Research and Technology Institute, Kinki University, Osaka; and [6]Department of Gastroenterological Surgery, Okayama University Graduate School of Medicine, Dentistry, and Pharmaceutical Sciences, Okayama, Japan

Note: Supplementary data for this article are available at Clinical Cancer Research Online (http://clincancerres.aacrjournals.org/).

Corresponding Author: Fuminori Sakurai, Department of Biochemistry and Molecular Biology, Graduate School of Pharmaceutical Sciences, Osaka University, Osaka, Japan. Phone: 81-6-6879-8188; Fax: 81-6-6879-8186; E-mail: sakurai@phs.osaka-u.ac.jp or Hiroyuki Mizuguchi, Department of Biochemistry and Molecular Biology, Graduate School of Pharmaceutical Sciences, Osaka University, 1-6 Yamadaoka, Suita, Osaka, 565-0871, Japan. Phone: 81-6-6879-8185, Fax: 81-6-6879-8186; E-mail: mizuguch@phs.osaka-u.ac.jp

doi: 10.1158/1078-0432.CCR-10-2008

Published OnlineFirst February 23, 2011; DOI:10.1158/1078-0432.CCR-10-2008

Translational Relevance

Oncolytic adenoviruses (Ad) are promising anticancer agents and have been used in human clinical trials. However, though a lesser extent than in tumor cells, some oncolytic Ads also replicate in normal human cells, resulting in unexpected toxicity. In this study, we included a microRNA (miRNA)-regulated posttranscriptional detargeting system into a telomerase-specific replication-competent Ad (TRAD), which has been used in clinical trials. Complementary sequences for miR-143, -145, and -199a, which have been shown to be exclusively downregulated in tumor cells, were inserted into the *E1* gene expression cassette. The TRAD containing these miRNA complementary sequences exhibited significantly reduced replication in normal cells (up to 1,000-fold reductions), including human primary cells, and comparable tumor cell lysis activity to the conventional TRAD. These results indicate that an miRNA-regulated posttranscriptional detargeting system offers a potential strategy to reduce the replication of TRAD in normal cells without altering tumor cell lysis activity, and makes it possible to increase the injected doses, leading to enhanced antitumor effects.

Ad (TRAD; also known as Telomelysin), which has an *E1* gene expression cassette driven by the human telomerase reverse transcriptase (hTERT) promoter, is one of the most promising oncolytic Ads (10, 11). A variety of tumor cells express telomerase and most normal cells do not, leading to tumor-selective efficient replication of TRAD. A phase I clinical trial using TRAD has already been carried out, and antitumor effects were shown in several patients (3). Combined therapy using anticancer agents and TRAD also has been shown to provide enhanced antitumor effects compared with either treatment alone (12). Another advantage of TRAD is that TRAD exerts antitumor effects on distant, uninjected tumors following intratumoral administration. TRAD efficiently replicates in the injected tumors and is disseminated from the injected tumors into the systemic circulation, resulting in infection of distant tumors with TRAD (11, 13). This property of TRAD has made it possible to visualize lymph mode metastasis by inclusion of the green fluorescence protein (GFP)-expression cassette into TRAD (14). However, these properties have led to the concern that TRAD also infects normal cells throughout the body after their dissemination from the injected tumors. Some oncolytic Ads, including TRAD, replicate to some extent in normal human cells although tumor-specific promoters are used probably because low levels of E1A expression can sufficiently support the replication of Ads (15). Previous studies have shown a more than 100-fold increase in Ad genome copy numbers in human primary fibroblasts 3 days after infection with TRAD (10, 11). Replication of TRAD in normal human cells might lead to unexpected cellular toxicity, therefore, in addition to a tumor-specific promoter, a system which can prevent the replication of TRAD in normal human cells should be incorporated into TRAD.

To achieve this goal, we utilized a microRNA (miRNA)-regulated gene expression system. MiRNAs are small noncoding RNAs of approximately 22-nt in length, and are endogenously expressed. MiRNAs bind to imperfectly complementary sequences in the 3′-untranslated region (UTR) of the target mRNA leading to the suppression of gene expression via posttranscriptional regulation. More than 800 miRNAs have been identified and have been shown to be expressed in tissue- and cell-type-specific patterns. Furthermore, recent studies have shown that several miRNAs, including miR-143, -145, and let-7, are specifically downregulated in tumor cells, compared with normal cells (16–20). Thus we hypothesized that incorporation of the complementary sequences for miRNAs selectively downregulated in tumor cells into the *E1* expression cassette would prevent the replication of TRADs in normal human cells without altering the antitumor effects.

In the present study, miR-143, -145, -199a, and let-7a were selected as the miRNAs exclusively downregulated in tumor cells. Four copies of sequences perfectly complementary to these miRNAs were inserted into the 3′-UTR of the *E1* gene expression cassette in TRADs. TRADs containing the target sequences for miR-143, -145, or -199a exhibited not only efficient oncolytic activities comparable to the parental TRAD, but also significantly reduced levels of replication (up to 1,000-fold reductions) in normal cells, including human primary cells. Furthermore, insertion of sequences complementary to liver-specific miR-122a into the *E1* gene expression cassette, in addition to the miR-199a target sequences, resulted in a decrease in virus replication in primary hepatocytes as well as other primary cells.

Materials and Methods

Cells

A549 (a human non–small cell lung cancer cell line), HepG2 (a human hepatocellular carcinoma cell line), and 293 cells (a transformed embryonic kidney cell line) were cultured in Dulbecco's modified Eagle's Medium containing 10% fetal bovine serum (FBS) and antibiotics. HT29 (a human colorectal cancer cell line) and WI38 cells (a normal human lung diploid fibroblast) were cultured in Minimum Essential Medium containing 10% FBS and antibiotics. H1299 cells (a human non–small cell lung cancer cell line) were cultured in RPMI1640 containing 10% FBS and antibiotics. These cell lines were obtained from the cell banks, including the Japanese Collection of Research Bioresources (JCRB) cell bank. The normal human lung fibroblasts (NHLF), normal human prostate stromal cells (PrSC), normal human small airway epithelial cells (SAEC), and normal human hepatocytes (Nhep; Lonza) were cultured in the medium recommended by the manufacturer.

Construction of TRADs

All TRADs were prepared by means of an improved *in vitro* ligation method described previously (21–23). hTERT promoter-driving *E1* gene-expressing shuttle plasmids having multiple tandem copies of sequences perfectly complementary to miRNAs in the 3′-UTR of the *E1* gene expression cassette were constructed as described below. A *KpnI*/*AflIII* fragment of pHMCMV5 (22) was ligated with oligonucleotides miR-143T-S1 and miR-143T-AS1, which contain miR-143 complementary sequences, resulting in pHMCMV5-143T-1. The sequences of the oligonucleotides are shown in Supplementary Table S1. Next, a *PacI*/*AflIII* fragment of pHMCMV5-143T-1 was ligated with oligonucleotides miR-143T-S2 and miR-143T-AS2. The resulting plasmid, pHMCMV5-143T, was digested with *I-CeuI* after digestion with *NheI* followed by *Klenow* treatment, and then ligated with the *I-CeuI*/*PmeI* fragment of pSh-hAIB (10), in which the *E1A* and *E1B* genes linked with an internal ribosomal entry site (IRES) are located downstream of the hTERT promoter, creating pSh-AIB-143T. For the construction of vector plasmids for TRADs, *I-CeuI*/*PI-SceI*-digested pSh-AIB-143T was ligated with the *I-CeuI*/*PI-SceI*-digested pAdHM3 (21), resulting in pAdHM3-AIB-143T. To generate TRADs, pAdHM3-AIB-143T was digested with *PacI* and was transfected into 293 cells using Superfect transfection reagent (Qiagen). All TRADs were propagated in 293 cells, purified by 2 rounds of cesium chloride gradient ultracentrifugation, dialyzed, and stored at −80°C. TRADs containing other miRNA complementary sequences were similarly constructed using the corresponding oligonucleotides (Supplementary Table S1). The parental TRAD was similarly prepared using pSh-AIB and pAdHM3. The virus particles (VP) and biological titers were determined by a spectrophotometrical method (24) and by using an Adeno-X rapid titer kit (Clontech), respectively. The ratio of particle-to-biological titer was between 6 and 9 for each TRAD used in this study.

Determination of miRNA expression levels in human normal and tumor cells

Total RNA, including miRNAs, was isolated from cells using Isogen (Nippon Gene). After quantification of the RNA concentration, miRNA levels were determined using a TaqMan MiRNA reverse transcription kit, TaqMan miRNA assay kit, and ABI Prism 7000 system (Applied Biosystems). Amplification of U6 served as an endogenous control to normalize the miRNA expression data.

Infection with TRADs

Cells were seeded into 24-well plates at 5×10^4 cells/well. On the following day, cells were infected with TRADs at a multiplicity of infection (MOI) of 0.4 or 2 (for cancer cell lines), or of 10 (for normal cells), for 2 hours. Following incubation for 3 (for cancer cell lines) or 5 days (for normal cells), total DNA, including viral genomic DNA, was isolated from the cells using a DNeasy Blood & Tissue Kit (Qiagen). After isolation, the Ad genomic DNA contents were quantified using an ABI Prism 7000 system (Applied Biosystems) as previously described (25). The Ad genome copy numbers were normalized by the copy numbers of glyceroaldehyde-3-phosphate-dehydrogenase (GAPDH). Cell viability was also examined by crystal violet staining and Alamar blue assay at the indicated time points. To examine the miRNA-specific suppression of TRAD replication in normal human cells, 50 nmol/L of 2′-*O*-methylated antisense oligonucleotide complementary to miR-143 or miR-199a (Gene Design Inc.) was transfected into normal cells using Lipofectamine 2000 (Invitrogen). Twenty-four hours after transfection, the cells were infected with TRADs and replication of TRADs was evaluated as described above.

Real-time reverse transcriptase PCR analysis for *E1A* gene expression

Cells were seeded as described above and were infected with TRADs at an MOI of 2 (for cancer cells) or 10 (for normal cells) for 1.5 hours. After a 24 hour-incubation, total RNA was isolated, and reverse transcription reaction was carried out using a SuperScript II First-Strand Synthesis System (Invitrogen). E1A mRNA levels were determined with the E1A-specific primers and probe using an ABI prism 7000 system (26). The E1A mRNA levels were normalized by the GAPDH mRNA levels.

Statistical analysis

Statistical significance ($P < 0.05$) was determined using Student's t test. Data are presented as means ± SD.

Results

Replication of the conventional TRAD in normal human cells

First, to examine replication of the conventional TRAD in normal human cells, WI38 cells, which are human embryonic lung fibroblasts, were infected with the conventional TRAD at an MOI of 2 or 10 (Fig. 1). The conventional TRAD did not highly replicate in WI38 cells at an MOI of 2; however, an almost 500-fold increase in the Ad genome

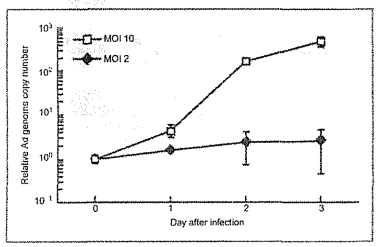

Figure 1. Replication of the conventional TRAD in WI38 cells. WI38 cells were infected with the conventional TRAD at an MOI of 2 or 10 for 2 hours. At the indicated time points, the copy numbers of the Ad genome and *GAPDH* gene were determined by real-time PCR. The ratio of the copy number of the Ad genome to that of GAPDH was normalized by the data on day 0. The data are shown as the means ± SD ($n = 3$).

Published OnlineFirst February 23, 2011; DOI:10.1158/1078-0432.CCR-10-2008

Downloaded from clincancerres.aacrjournals.org on May 11, 2011
Copyright © 2011 American Association for Cancer Research

Published OnlineFirst February 23, 2011; DOI:10.1158/1078-0432.CCR-10-2008

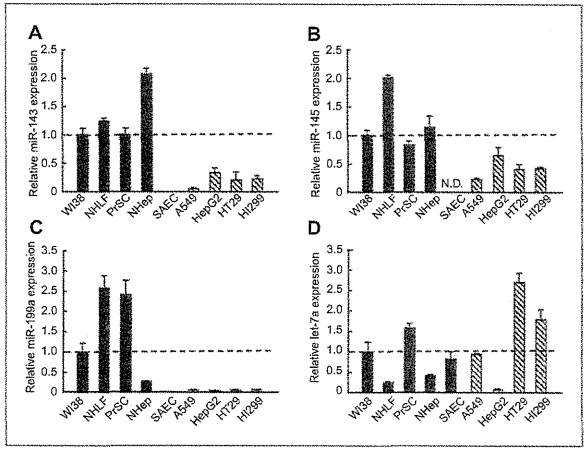

Figure 2. MiRNA expression levels in the human normal (solid bar) and tumor cells (hatched bar). MiRNA expression was determined by real-time RT-PCR. The ratio of miRNA to U6 expression levels was normalized by the data of WI38 cells. The data are shown as the means ± SD ($n = 3$). N.D., not detected.

was found 3 days after infection at an MOI of 10. These data indicate that the conventional TRAD replicates in normal human cells at a high MOI, even though tumor-specific hTERT promoters are used for the *E1* gene expression.

MiRNA expression levels in human tumor and normal cells

To examine the expression levels of miR-143, -145, -199a, and let-7a in the human normal and tumor cells, reverse transcriptase PCR (RT-PCR) analysis was carried out. Several studies have shown that these miRNAs are downregulated in various types of tumor cells isolated from cancer patients, compared with the corresponding normal tissues (16–18, 27). The expression levels of miR-143, -145, and -199a in the tumor cells were approximately 2- to 100-fold lower than those in the normal cells, although SAECs expression levels of miR-143, -145, and -199a were comparable or lower than those in the tumor cells (Fig. 2). In particular, a large reduction was found for miR-199a expression in all tumor cells, compared with the normal cells. On the other hand, the expression levels of let-7a in HT29 and H1299 cells were higher than those in the normal cells, although HepG2 cells expressed lower levels of let-7a than the normal cells. The absolute amounts of let-7a were more than 10-fold higher than those of the other miRNAs in all tumor and normal cells, except for NHLF, NHep, and HepG2 cells (data not shown).

Development of TRADs carrying an miRNA-regulated *E1* gene expression system

Next, to develop TRADs carrying a miRNA-regulated *E1* gene expression cassette (TRAD-miRT), we incorporated 4 copies of the perfectly complementary sequences for miR-143, -145, -199a, or let-7a into the 3′-UTR of the *E1* gene expression cassette (Fig. 3A). In TRADs, the *E1A* gene was connected with the *E1B* gene via IRES. We found that the expression of both the first and second gene in the IRES-containing expression cassette was suppressed in an miRNA-dependent manner by insertion of the miR-122a complementary sequences into the region downstream of the second gene in miR-122a-expressing Huh-7 cells, not in HepG2 cells, which express a low level of miR-122a (Supplementary Fig. S1), although it remains controversial whether miRNA-mediated posttranscriptional regulation can occur in an IRES-containing expression cassette (28–30). All TRADs were efficiently grown in normal 293 cells, and the ratios of infectious titers to physical titers were comparable among all the TRADs, including the parental TRAD.

Tumor cell lysis activity and replication of TRAD-miRT in tumor cells

To examine whether or not the inclusion of the sequences complementary to the miRNAs downregulated in tumor cells would inhibit the tumor cell lysis activity of TRADs, the viability of tumor cells was evaluated after infection with the TRADs. Almost all tumor cells were lysed by TRAD-143T, -145T, and -199aT at 3 days after infection, although cell lysis by TRAD-let7aT was largely inhibited (Fig. 3B). Furthermore, time-course studies of cell viability showed that TRAD-143T, -145T, and -199aT exhibited cytopathic efficacies comparable to that of the parental TRAD in the tumor cells at an MOI of 0.4 (Fig. 3C). Similar results were obtained at an MOI of 2 (data not shown).

Published OnlineFirst February 23, 2011; DOI:10.1158/1078-0432.CCR-10-2008

We next examined the replication ability of the TRADs in the tumor cells by determining the viral genome copy numbers. TRAD-143T, -145T, and -199aT efficiently replicated in the tumor cells, and the viral genome copy numbers of TRAD-143T, -145T, and -199aT in the tumor cells were more than 500-fold higher than those in the normal cells (data not shown). In addition, TRAD-143T, -145T, and -199aT exhibited viral genome copy numbers similar to that of the conventional TRAD in all tumor cells (Fig. 3D). All TRADs except for TRAD-let7aT also expressed similar levels of E1A mRNA (Fig. 3E). In contrast, insertion of let-7a complementary sequences largely inhibited the replication in all tumor cells. The E1A mRNA level was also reduced by 42% in H1299 cells infected with TRAD-let7aT. Inefficient replication of TRAD-let7aT in the tumor cells corresponded to the low cytopathic effects described above. These results indicate that TRADs containing the complementary sequences for miR-143, -145, or -199a exhibit efficient *E1* gene expression in the tumor cells and tumor cell lysis activity comparable to those of the conventional TRAD.

Reduced replication of TRAD-miRT in normal cells

To examine whether replication of TRADs in normal cells is suppressed by incorporation of the sequences complementary to the miRNAs downregulated in tumor cells, normal human cells were infected with the TRADs. The virus genome copy numbers of TRAD-143T, -145T, and -199aT were 5- to 1,000-fold reduced, compared with the conventional TRAD at 5 days following infection in WI38 cells (Fig. 4A). An approximately 3- to 300-fold reduction in the genome copy numbers of TRAD-143T, -145T, and -199aT was also observed in NHLF and PrSC. The replication of TRADs was also suppressed in SAEC by the insertion of the miRNA complementary sequences, although the expression levels of miR-143, -145, and -199a in SAEC were much lower than those in the other normal cells (Fig. 2). The suppressive effects of insertion of the miRNA target sequences were different among the cells; however, overall, the insertion of miR-199a complementary sequences mediated similar or higher suppressive effects on the replication of TRADs in all the normal cells examined, compared with insertion of the sequences complementary to miR-143 and -145. Replication of TRAD-199aT was inhibited by more than 10-fold in all the normal cells except for SAEC. We also examined the viabilities of the normal cells after infection with the TRADs. No apparent differences in cell viabilities were found among the TRADs by crystal violet staining (data not shown); however, Alamar blue assay showed that the average values of the normal cell viabilities were higher after infection with TRAD-miRT than after infection with the conventional TRAD (Fig. 4B). These results suggest that the suppression of TRAD replication by insertion of the miRNA complementary sequences results in the improvement of the TRAD safety profile in normal cells.

Next, to evaluate whether the reduction in replication of TRAD-miRT was miRNA-dependent, miRNAs were inhibited by a 2′-*O*-methylated antisense oligonucleotide. NHLF and PrSC cells were transfected with the 2′-*O*-methylated antisense oligonucleotide against miR-143 or -199a, and then the cells were infected with the TRADs, 24 hour after transfection. In the cells transfected with the 2′-*O*-methylated antisense oligonucleotide against miR-143 or -199a, the reduction in the replication of TRAD-miRT was significantly restored, but the scramble 2′-*O*-methylated oligonucleotide did not significantly affect the replication of TRAD-miRT (Fig. 4C). These results indicate that the reduction in the replication of TRAD-miRT in the normal cells was miRNA-dependent.

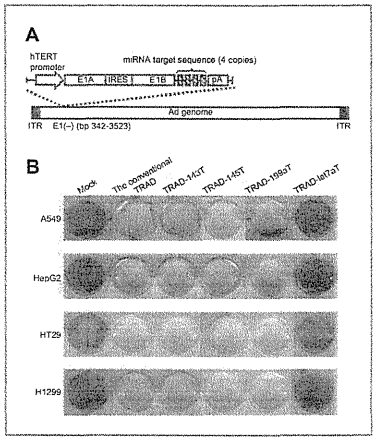

Figure 3. Replication and oncolytic activity of TRADs containing the miRNA complementary sequences in the tumor cells. A, a schematic diagram of a TRAD containing the miRNA-regulated *E1* gene expression system. ITR: inverted terminal repeat. B, crystal violet analysis of the cytopathic effects of TRADs in the tumor cells. The cells were infected with the TRADs at an MOI of 2 for 2 hours. Three days after infection, the cells were stained with crystal violet. The results are representative of at least 2 independent experiments. C, time-course study of the tumor cell lysis activity of TRADs by Alamar blue assay. The cells were infected with the TRADs at an MOI of 0.4 for 2 hours. At the indicated time points, the viability of the cells was analyzed by Alamar blue assay. The data were normalized by the data of the mock-infected group. D, the viral genome copy numbers of TRADs in the tumor cells. The cells were infected with the TRADs at an MOI of 2 for 2 hours. Three days after infection, the viral genome copy numbers were quantified by real-time PCR. The data was normalized by the data of the conventional TRAD group. E, the E1A mRNA levels in H1299 cells 24 hour after infection with the TRADs. The cells were infected with the TRADs at an MOI of 2 for 1.5 hours. Twenty-four hours after infection, the E1A mRNA levels were determined by real-time RT-PCR. The data was normalized by the data of the conventional TRAD group. All the data are shown as the means ± SD ($n = 3$–6). *, $P < 0.05$; **, $P < 0.005$.

Published OnlineFirst February 23, 2011; DOI:10.1158/1078-0432.CCR-10-2008

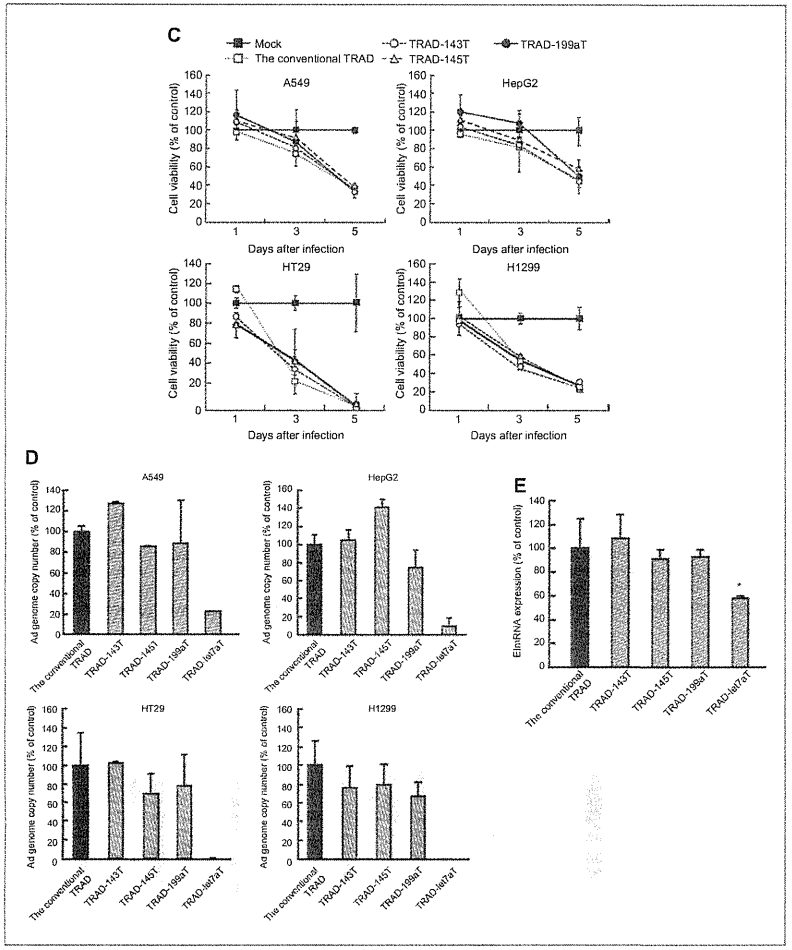

Figure 3. (*Continued*)

Published OnlineFirst February 23, 2011; DOI:10.1158/1078-0432.CCR-10-2008

Figure 4. Reduced replication of TRADs in normal human cells by insertion of the miRNA complementary sequences. A, the viral genome copy numbers of TRADs in normal cells. The cells were infected with the TRADs at an MOI of 10 for 2 hours. Five days after infection, the viral genome copy numbers were determined by real-time PCR. B, time-course study of the normal human cell viabilities after infection with TRADs by Alamar blue assay. The cells were infected with the TRADs at an MOI of 10 for 2 hours. At the indicated time points, the viability of the cells was analyzed by Alamar blue assay. The data were normalized by the data of the mock-infected group. C, restoration of TRAD replication in human normal cells by 2′-O-methylated antisense oligonucleotides. The cells were transfected with 50 nmol/L of 2′-O-methylated antisense oligonucleotides for miR-143 or -199a. Twenty-four hours after transfection, the cells were infected with the TRADs at an MOI of 10, and the viral genome copy numbers were determined 5 days after infection with the TRADs. D, the E1A mRNA levels in normal human cells. The cells were infected with the TRADs at an MOI of 10 for 1.5 hours. Twenty-four hours after infection, the E1 mRNA levels were determined by real-time RT-PCR. The data was normalized by the data of the conventional TRAD group. All the data are shown as the means ± SD ($n = 3$–4). *, $P < 0.05$; **, $P < 0.005$.

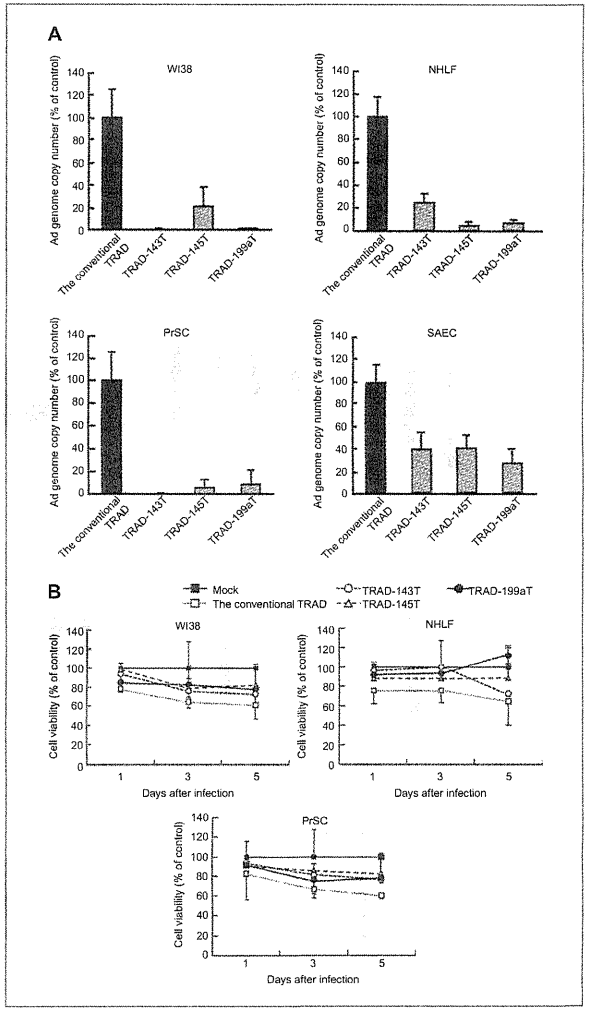

Downloaded from clincancerres.aacrjournals.org on May 11, 2011
Copyright © 2011 American Association for Cancer Research

Published OnlineFirst February 23, 2011; DOI:10.1158/1078-0432.CCR-10-2008

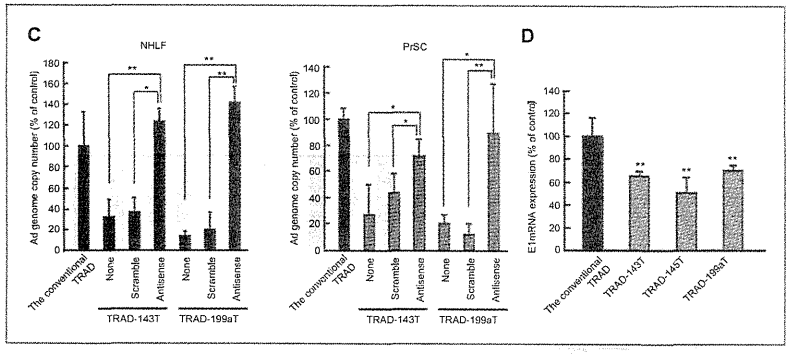

Figure 4. (*Continued*)

E1A expression by TRAD-miRT in normal cells

To determine whether incorporation of the miRNA complementary sequences into the *E1* gene expression cassette decreases the *E1* mRNA levels in normal human cells, real-time RT-PCR analysis for the E1A mRNA levels wascarried out. The E1A mRNA levels were reduced by more than 30% for TRAD-143T, -145T, and -199aT, compared with the parent TRAD, in NHLF (Fig. 4D). The reduction in the E1A mRNA levels corresponded to the suppression in replication of TRAD-miRT, indicating that miRNA-mediated reduction in the *E1* gene expression resulted in a reduced replication of TRAD-miRT.

Development of TRADs containing the complementary sequences for liver-specific miRNA

To prevent the replication of TRADs in liver hepatocytes as well as other normal cells, we incorporated not only miR-199a complementary sequences but also sequences complementary to liver-specific miR-122a into the *E1* gene expression cassette, resulting in TRAD-122a/199aT (Fig. 5A). It is well known that Ads have high hepatic tropism, leading to efficient liver accumulation even after local administration. MiR-122a was expressed approximately 100- and 20-fold more abundantly in NHep and Huh-7 cells, respectively, than in the other normal human cells and tumor cells (Fig. 5B); conversely, the other normal cells expressed more than 10-fold lower levels of miR-122a than miR-143, -145, and -199a (data not shown). Incorporation of miR-122a complementary sequences alone significantly reduced the virus genome copy number of TRAD-122aT in NHLF and NHep; however, no statistically significant decrease in the genome copy number of TRAD-122aT was found in PrSC (Fig. 5C). On the other hand, insertion of miR-199a target sequences alone was less efficient than insertion of miR-122a target sequences in NHep, probably due to the lower expression of miR-199a than miR-122a in NHep. By contrast, insertion of both miR-122a and miR-199a target sequences into the *E1* gene expression cassette efficiently reduced the replication of TRAD-122a/199aT by 10- to 50-fold in all normal cells examined. Significantly reduced replication of TRAD-122a and TRAD-122a/199aT was also found in Huh-7 cells, which are a hepatoma cell line highly expressing miR-122a and are often used as a model of hepatocytes (Supplementary Fig. S2). The incorporation of the miR-145 complementary sequences was also effective for suppressing the TRAD replication in NHep (Supplementary Fig. S3). The E1A mRNA levels were reduced for TRAD-122aT and -122a/199aT in NHep (Fig. 5D). In addition, TRAD-122a/199aT efficiently replicated in the tumor cells, resulting in efficient tumor cell lysis (Fig. 5E and F). These results indicate that replication of the TRADs in various types of normal human cells, including liver hepatocytes, is significantly reduced by insertion of the multiple target sequences to both miR-122a and -199a, without influencing the tumor cell lysis activity.

Discussion

The aim of this study was to prevent the replication of TRADs in normal human cells by incorporation of sequences complementary to miRNAs that are selectively downregulated in tumor cells, without altering the tumor cell lysis activity. Currently, there is no appropriate animal model which fully supports the *in vivo* replication of Ads and evaluation of the *in vivo* toxicity caused by oncolytic Ads, and thus it is important to be cautious in regard to oncolytic Ad-induced toxicity. To prevent the *E1* gene expression and replication of oncolytic Ads in normal cells as much as possible, an miRNA-mediated posttranscriptional detargeting system was included in TRADs, in addition to the transcriptional targeting system via tumor-specific promoters.

Published OnlineFirst February 23, 2011; DOI:10.1158/1078-0432.CCR-10-2008

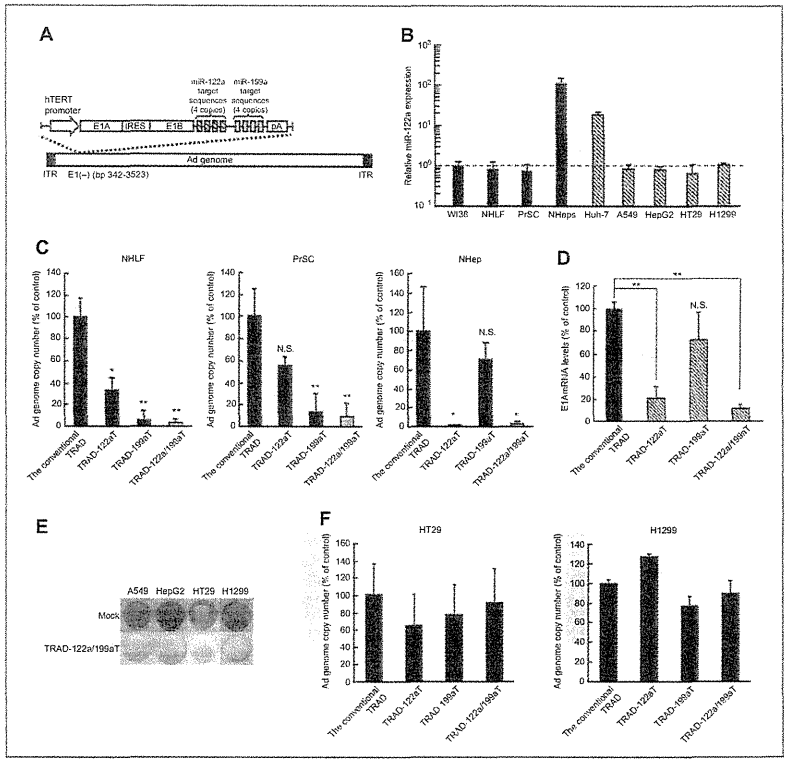

Figure 5. Tumor cell lysis activity and enhanced safety profile of TRAD-122a/199aT. A, a schematic diagram of TRAD-122a/199aT. B, miR-122a expression levels in the normal and tumor cells. C, the viral genome copy numbers of TRAD-122a/199aT in normal human cells. D, the E1A mRNA levels in NHep. E, crystal violet analysis for the cytopathic effects of TRAD-122a/199aT. The results are representative of 2 independent experiments. F, the viral genome copy numbers of TRAD-122a/199aT in tumor cells. The tumor and normal cells were infected with the TRADs at an MOI of 2 (tumor cells) or 10 (normal cells) for 2 hours. The cells were stained with crystal violet 3 days after infection. The viral genome copy numbers were determined 3 (tumor cells) or 5 days (normal cells) after infection. For determination of the E1A mRNA levels, total RNA was isolated from NHep 24 hour after infection with the TRADs at an MOI of 10, and the E1A mRNA levels were determined by real-time RT-PCR. The data was normalized by the data of the conventional TRAD group. All the data are shown as the means ± SD ($n = 3$–6). N.S.: not significantly different. *, $P < 0.05$; **, $P < 0.005$.

As described above, TRAD replicates in the injected tumors and is disseminated from the injected tumors into the systemic circulation, leading to infection of distant, uninjected tumors (11, 13, 14). This property of TRAD had led to a concern that TRAD could infect normal cells over the whole body, including the hepatocytes, after dissemination from the injected tumors. It is crucial that such unexpected infection of normal cells by TRAD is prevented. Previous studies have shown that insertion of sequences complementary to liver-specific miR-122a reduced the replication of oncolytic Ads in Huh-7 cells, which are a model cell for hepatocytes (31–33). It is especially crucial

Published OnlineFirst February 23, 2011; DOI:10.1158/1078-0432.CCR-10-2008

to prevent the replication of TRAD in the liver, because Ad vectors have strong hepatotropism. However, TRAD also might infect normal cells other than hepatocytes, indicating that replication of oncolytic Ads in normal cells other than hepatocytes should also be suppressed. To prevent the replication of TRADs in other normal cells, we incorporated the sequences complementary to miR-143, -145, -199a, or let-7a, which are downregulated in the tumors and widely expressed in normal cells. The expression levels of these miRNAs in the tumor cells were lower than those in the normal cells in this study, and insertion of sequences complementary to miR-143, -145, or -199a significantly reduced the E1A mRNA levels and the replication of TRADs in the normal cells.

Overall, among the miRNA complementary sequences, the miR-199a complementary sequences appeared to be the most efficient at suppressing the replication of TRADs across all the normal cells except for hepatocytes; however, insertion of miR-199a target sequences alone failed to significantly reduce the replication of TRADs in the hepatocytes. To simultaneously prevent the replication of TRADs in various types of normal cells, including hepatocytes, we incorporated sequences complementary to miR-122a, which is abundantly expressed in hepatocytes, in addition to miR-199a target sequences. Brown and colleagues reported that a desired transgene expression pattern was achieved, depending on the miRNA expression profile, by incorporation of target sequences for 2 distinct miRNAs (34). TRAD-122aT/199aT exhibited more than 10-fold reduction in the replication in all the normal cells except for SAEC, although insertion of target sequences for miR-122a or miR-199a alone failed to suppress the replication of TRADs in either of the normal cells. Furthermore, TRAD-122aT/199aT and the parental TRAD mediated similar cytopathic efficacies in the tumor cells. These results indicate that replication of TRADs in not only hepatocytes but also other normal cells is simultaneously reduced by insertion of both miR-122a complementary sequences and sequences complementary to miRNAs highly expressed in normal cells, without altering the tumor cell lysis activity.

TRADs containing miR-122a complementary sequences are also considered to be promising for the treatment of liver cancer because miR-122a is significantly downregulated in liver cancer cells (35–37) leading to efficient replication and lytic activity of TRADs containing miR-122a complementary sequences in liver cancer cells. This study has shown that TRAD-122aT/199aT caused efficient cell lysis in a hepatocellular carcinoma cell line, HepG2 cells, while the replication of TRADs containing the miR-122a complementary sequences in normal hepatocytes, which highly express miR-122a, was significantly inhibited.

The expression levels of miRNAs are a crucial factor to suppress the gene expression by miRNAs. Brown and colleagues showed that miRNAs should be expressed at a concentration above the threshold (>100 copies/pg small RNA) to induce miRNA-regulated suppression of transgene expression (34). We were not able to precisely show the expression levels of miRNAs as the ratio of copies/pg small RNA in this study; however, comparing the miRNA levels in this study with those reported by Brown and colleagues (34), we consider that the expression levels of miR-143, -145, and -199a in the normal cells were higher than 100 copies/pg small RNA, leading to efficient suppression of the replication of TRADs.

Several studies have shown that let-7, including let-7a, is significantly downregulated in tumor cells (16, 19, 20). Edge and colleagues reported that insertion of let-7a complementary sequences into the matrix protein expression cassette of the vesicular somatitis virus (VSV) suppressed the replication of VSV in human primary fibroblast MG38 cells; on the other hand, VSV carrying let-7a target sequences efficiently replicated in A549 cells (38). However, our data showed that cancer cell lines other than HepG2 cells expressed similar or higher levels of let-7a than the normal cells. In addition, the expression levels of let-7a were more than 10-fold higher than those of the other miRNAs in the tumor cells. Abundant let-7a expression leads to a reduction in the replication of TRAD-let7aT in tumor cells. Furthermore, the members of the let-7 family, including let-7b and let-7c, have the same seed sequence, suggesting that let-7 family members other than let-7a would also contribute to the significant suppression of replication of TRAD-let7aT. These results suggest that not only expression profiles of miRNAs but also absolute amounts of miRNA expression in the cells are of great importance for miRNA-regulated gene expression.

Our data showed that the E1A mRNA levels were reduced by approximately 30% to 50% for TRAD-143T, -145T, and -199aT, compared with the conventional TRAD 24 hour after infection with the normal cells. These reduction levels in the E1A mRNA were much smaller than those in the Ad genome copy numbers at 5 days after infection; however, these reductions in the E1A mRNA levels would lead to large differences in the Ad genome copy numbers after several virus replication cycles. More than 5-fold reductions in the E1A mRNA were found for TRAD-143T, -145T, and -199aT, compared with the parental TRAD, 5 days after infection with the normal cells (data not shown).

A phase I clinical trial of the parental TRAD was conducted, and serious adverse events were not observed (3). In this study, efficient replication of the conventional TRAD in WI38 cells was found at an MOI of 10; however, the conventional TRAD did not exhibit a high level of replication at an MOI of 2. It might be unlikely that such a high titer (MOI 10) of oncolytic Ad would infect organs distal from the injection points in clinical trials; however, normal cells around the injection points might be infected with a high titer of oncolytic Ad. In addition, even though no apparent replication of TRADs is observed in normal cells after infection of TRADs, the expression of Ad proteins, including E1A and E4 proteins, affects the cellular functions via various mechanisms (39–41). This study indicates that inclusion of an miRNA-regulated *E1* gene expression system in oncolytic Ads enhances the safety of oncolytic Ads and makes it possible to increase the injection doses, leading to superior therapeutic effects.

Published OnlineFirst February 23, 2011; DOI:10.1158/1078-0432.CCR-10-2008

In summary, we developed TRADs in which the *E1* gene expression is controlled by miRNAs more highly expressed in normal cells than tumor cells. The TRADs containing the sequences complementary to miR-143, -145, or -199a exhibited reduced replication in the normal cells without altering the tumor cell lysis activity. Furthermore, incorporation of both miR-199a and miR-122a target sequences significantly suppressed the replication in all human primary cells examined, including hepatocytes. TRAD-miRT has enhanced both the safety profiles and comparable tumor cell lysis activity to the parental TRAD, suggesting that TRAD-miRT offers great potential for the treatment of tumors.

Disclosure of Potential Conflicts of Interest

Toshiyoshi Fujiwara and Hiroyuki Mizuguchi are consultants to Oncolys BioPharma, Inc. No other potential conflicts of interest were disclosed.

References

1. Mathis JM, Stoff-Khalili MA, Curiel DT. Oncolytic adenoviruses—selective retargeting to tumor cells. Oncogene 2005;24:7775–91.
2. Ribacka C, Pesonen S, Hemminki A. Cancer, stem cells, and oncolytic viruses. Ann Med 2008;40:496–505.
3. Nemunaitis J, Tong AW, Nemunaitis M, Senzer N, Phadke AP, Bedell C, et al. A phase I study of telomerase-specific replication competent oncolytic adenovirus (telomelysin) for various solid tumors. Mol Ther 2010;18:429–34.
4. Li JL, Liu HL, Zhang XR, Xu JP, Hu WK, Liang M, et al. A phase I trial of intratumoral administration of recombinant oncolytic adenovirus overexpressing HSP70 in advanced solid tumor patients. Gene Ther 2009;16:376–82.
5. Freytag SO, Movsas B, Aref I, Stricker H, Peabody J, Pegg J, et al. Phase I trial of replication-competent adenovirus-mediated suicide gene therapy combined with IMRT for prostate cancer. Mol Ther 2007;15:1016–23.
6. Li Y, Yu DC, Chen Y, Amin P, Zhang H, Nguyen N, et al. A hepatocellular carcinoma-specific adenovirus variant, CV890, eliminates distant human liver tumors in combination with doxorubicin. Cancer Res 2001;61:6428–36.
7. Rodriguez R, Schuur ER, Lim HY, Henderson GA, Simons JW, Henderson DR. Prostate attenuated replication competent adenovirus (ARCA) CN706: a selective cytotoxic for prostate-specific antigen-positive prostate cancer cells. Cancer Res 1997;57:2559–63.
8. Matsubara S, Wada Y, Gardner TA, Egawa M, Park MS, Hsieh CL, et al. A conditional replication-competent adenoviral vector, Ad-OC-E1a, to cotarget prostate cancer and bone stroma in an experimental model of androgen-independent prostate cancer bone metastasis. Cancer Res 2001;61:6012–9.
9. Yamamoto M, Davydova J, Wang M, Siegal GP, Krasnykh V, Vickers SM, et al. Infectivity enhanced, cyclooxygenase-2 promoter-based conditionally replicative adenovirus for pancreatic cancer. Gastroenterology 2003;125:1203–18.
10. Kawashima T, Kagawa S, Kobayashi N, Shirakiya Y, Umeoka T, Teraishi F, et al. Telomerase-specific replication-selective virotherapy for human cancer. Clin Cancer Res 2004;10:285–92.
11. Taki M, Kagawa S, Nishizaki M, Mizuguchi H, Hayakawa T, Kyo S, et al. Enhanced oncolysis by a tropism-modified telomerase-specific replication-selective adenoviral agent OBP-405 ('Telomelysin-RGD'). Oncogene 2005;24:3130–40.
12. Watanabe T, Hioki M, Fujiwara T, Nishizaki M, Kagawa S, Taki M, et al. Histone deacetylase inhibitor FR901228 enhances the antitumor effect of telomerase-specific replication-selective adenoviral agent OBP-301 in human lung cancer cells. Exp Cell Res 2006;312:256–65.
13. Umeoka T, Kawashima T, Kagawa S, Teraishi F, Taki M, Nishizaki M, et al. Visualization of intrathoracically disseminated solid tumors in mice with optical imaging by telomerase-specific amplification of a transferred green fluorescent protein gene. Cancer Res 2004;64:6259–65.
14. Kishimoto H, Kojima T, Watanabe Y, Kagawa S, Fujiwara T, Uno F, et al. In vivo imaging of lymph node metastasis with telomerase-specific replication-selective adenovirus. Nat Med 2006;12:1213–9.
15. Hitt MM, Graham FL. Adenovirus E1A under the control of heterologous promoters: wide variation in E1A expression levels has little effect on virus replication. Virology 1990;179:667–78.
16. Takamizawa J, Konishi H, Yanagisawa K, Tomida S, Osada H, Endoh H, et al. Reduced expression of the let-7 microRNAs in human lung cancers in association with shortened postoperative survival. Cancer Res 2004;64:3753–6.
17. Michael MZ, SM OC, van Holst Pellekaan NG, Young GP, James RJ. Reduced accumulation of specific microRNAs in colorectal neoplasia. Mol Cancer Res 2003;1:882–91.
18. Slaby O, Svoboda M, Fabian P, Smerdova T, Knoflickova D, Bednarikova M, et al. Altered expression of miR-21, miR-31, miR-143 and miR-145 is related to clinicopathologic features of colorectal cancer. Oncology 2007;72:397–402.
19. Yanaihara N, Caplen N, Bowman E, Seike M, Kumamoto K, Yi M, et al. Unique microRNA molecular profiles in lung cancer diagnosis and prognosis. Cancer Cell 2006;9:189–98.
20. Johnson SM, Grosshans H, Shingara J, Byrom M, Jarvis R, Cheng A, et al. RAS is regulated by the let-7 microRNA family. Cell 2005;120:635–47.
21. Mizuguchi H, Kay MA. Efficient construction of a recombinant adenovirus vector by an improved in vitro ligation method. Hum Gene Ther 1998;9:2577–83.
22. Mizuguchi H, Kay MA. A simple method for constructing E1- and E1/E4-deleted recombinant adenoviral vectors. Hum Gene Ther 1999;10:2013–7.
23. Sakurai F, Kawabata K, Yamaguchi T, Hayakawa T, Mizuguchi H. Optimization of adenovirus serotype 35 vectors for efficient transduction in human hematopoietic progenitors: comparison of promoter activities. Gene Ther 2005;12:1424–33.
24. Maizel JV Jr, White DO, Scharff MD. The polypeptides of adenovirus. I. Evidence for multiple protein components in the virion and a comparison of types 2, 7A, and 12. Virology 1968;36:115–25.
25. Koizumi N, Kawabata K, Sakurai F, Watanabe Y, Hayakawa T, Mizuguchi H. Modified adenoviral vectors ablated for coxsackievirus-adenovirus receptor, alphav integrin, and heparan sulfate binding reduce in vivo tissue transduction and toxicity. Hum Gene Ther 2006;17:264–79.
26. Ishii-Watabe A, Uchida E, Iwata A, Nagata R, Satoh K, Fan K, et al. Detection of replication-competent adenoviruses spiked into recombinant adenovirus vector products by infectivity PCR. Mol Ther 2003;8:1009–16.

Acknowledgments

We thank Takako Ichinose, Koyori Yano (National Institute of Biomedical Innovation, Osaka, Japan), and Sayuri Okamoto (Graduate School of Pharmaceutical Sciences, Osaka University, Osaka, Japan) for their help.

Grant Support

Support was received from a grant-in-aid for Young Scientists (A) F. Sakurai from the Ministry of Education, Culture, Sports, Science, and Technology (MEXT) of Japan (F. Sakurai), and a grant from the Takeda Science Foundation (H. Mizuguchi).

The costs of publication of this article were defrayed in part by the payment of page charges. This article must therefore be hereby marked *advertisement* in accordance with 18 U.S.C. Section 1734 solely to indicate this fact.

Received July 28, 2010; revised November 18, 2010; accepted December 14, 2010; published OnlineFirst February 23, 2011.

Downloaded from clincancerres.aacrjournals.org on May 11, 2011
Copyright © 2011 American Association for Cancer Research

Published OnlineFirst February 23, 2011; DOI:10.1158/1078-0432.CCR-10-2008

27. Iorio MV, Visone R, Di Leva G, Donati V, Petrocca F, Casalini P, et al. MicroRNA signatures in human ovarian cancer. Cancer Res 2007;67:8699–707.
28. Mathonnet G, Fabian MR, Svitkin YV, Parsyan A, Huck L, Murata T, et al. MicroRNA inhibition of translation initiation in vitro by targeting the cap-binding complex eIF4F. Science 2007;317:1764–7.
29. Petersen CP, Bordeleau ME, Pelletier J, Sharp PA. Short RNAs repress translation after initiation in mammalian cells. Mol Cell 2006;21:533–42.
30. Pillai RS, Bhattacharyya SN, Artus CG, Zoller T, Cougot N, Basyuk E, et al. Inhibition of translational initiation by Let-7 MicroRNA in human cells. Science 2005;309:1573–6.
31. Cawood R, Chen HH, Carroll F, Bazan-Peregrino M, van Rooijen N, Seymour LW. Use of tissue-specific microRNA to control pathology of wild-type adenovirus without attenuation of its ability to kill cancer cells. PLoS Pathog 2009;5:e1000440.
32. Leja J, Nilsson B, Yu D, Gustafson E, Akerstrom G, Oberg K, et al. Double-detargeted oncolytic adenovirus shows replication arrest in liver cells and retains neuroendocrine cell killing ability. PLoS One 2010;5:e8916.
33. Ylosmaki E, Hakkarainen T, Hemminki A, Visakorpi T, Andino R, Saksela K. Generation of a conditionally replicating adenovirus based on targeted destruction of E1A mRNA by a cell type-specific MicroRNA. J Virol 2008;82:11009–15.
34. Brown BD, Gentner B, Cantore A, Colleoni S, Amendola M, Zingale A, et al. Endogenous microRNA can be broadly exploited to regulate transgene expression according to tissue, lineage and differentiation state. Nat Biotechnol 2007;25:1457–67.
35. Coulouam C, Factor VM, Andersen JB, Durkin ME, Thorgeirsson SS. Loss of miR-122 expression in liver cancer correlates with suppression of the hepatic phenotype and gain of metastatic properties. Oncogene 2009;28:3526–36.
36. Bai S, Nasser MW, Wang B, Hsu SH, Datta J, Kutay H, et al. MicroRNA-122 inhibits tumorigenic properties of hepatocellular carcinoma cells and sensitizes these cells to sorafenib. J Biol Chem 2009;284:32015–27.
37. Gramantieri L, Ferracin M, Fornari F, Veronese A, Sabbioni S, Liu CG, et al. Cyclin G1 is a target of miR-122a, a microRNA frequently downregulated in human hepatocellular carcinoma. Cancer Res 2007;67:6092–9.
38. Edge RE, Falls TJ, Brown CW, Lichty BD, Atkins H, Bell JC. A let-7 MicroRNA-sensitive vesicular stomatitis virus demonstrates tumor-specific replication. Mol Ther 2008;16:1437–43.
39. Duerksen-Hughes P, Wold WS, Gooding LR. Adenovirus E1A renders infected cells sensitive to cytolysis by tumor necrosis factor. J Immunol 1989;143:4193–200.
40. Ramalingam R, Worgall S, Rafii S, Crystal RG. Downregulation of CXCR4 gene expression in primary human endothelial cells following infection with E1(-)E4(-) adenovirus gene transfer vectors. Mol Ther 2000;2:381–6.
41. Weitzman MD. Functions of the adenovirus E4 proteins and their impact on viral vectors. Front Biosci 2005;10:1106–17.

OPEN ACCESS Freely available online PLoS one

Efficient and Directive Generation of Two Distinct Endoderm Lineages from Human ESCs and iPSCs by Differentiation Stage-Specific SOX17 Transduction

Kazuo Takayama[1,2], Mitsuru Inamura[1,2], Kenji Kawabata[2,3], Katsuhisa Tashiro[2], Kazufumi Katayama[1], Fuminori Sakurai[1], Takao Hayakawa[4,5], Miho Kusuda Furue[6,7], Hiroyuki Mizuguchi[1,2,8]*

1 Laboratory of Biochemistry and Molecular Biology, Graduate School of Pharmaceutical Sciences, Osaka University, Suita, Osaka, Japan, **2** Laboratory of Stem Cell Regulation, National Institute of Biomedical Innovation, Ibaraki, Osaka, Japan, **3** Laboratory of Biomedical Innovation, Graduate School of Pharmaceutical Sciences, Osaka University, Suita, Osaka, Japan, **4** Pharmaceutics and Medical Devices Agency, Chiyoda-ku, Tokyo, Japan, **5** Pharmaceutical Research and Technology Institute, Kinki University, Higashiosaka, Osaka, Japan, **6** JCRB Cell Bank, Division of Bioresources, National Institute of Biomedical Innovation, Ibaraki, Osaka, Japan, **7** Laboratory of Cell Processing, Institute for Frontier Medical Sciences, Kyoto University, Sakyo-ku, Kyoto, Japan, **8** The Center for Advanced Medical Engineering and Informatics, Osaka University, Suita, Osaka, Japan

Abstract

The establishment of methods for directive differentiation from human embryonic stem cells (ESCs) and induced pluripotent stem cells (iPSCs) is important for regenerative medicine. Although Sry-related HMG box 17 (SOX17) overexpression in ESCs leads to differentiation of either extraembryonic or definitive endoderm cells, respectively, the mechanism of these distinct results remains unknown. Therefore, we utilized a transient adenovirus vector-mediated overexpression system to mimic the SOX17 expression pattern of embryogenesis. The number of alpha-fetoprotein-positive extraembryonic endoderm (ExEn) cells was increased by transient SOX17 transduction in human ESC- and iPSC-derived primitive endoderm cells. In contrast, the number of hematopoietically expressed homeobox (HEX)-positive definitive endoderm (DE) cells, which correspond to the anterior DE *in vivo*, was increased by transient adenovirus vector-mediated SOX17 expression in human ESC- and iPSC-derived mesendoderm cells. Moreover, hepatocyte-like cells were efficiently generated by sequential transduction of SOX17 and HEX. Our findings show that a stage-specific transduction of SOX17 in the primitive endoderm or mesendoderm promotes directive ExEn or DE differentiation by SOX17 transduction, respectively.

Citation: Takayama K, Inamura M, Kawabata K, Tashiro K, Katayama K, et al. (2011) Efficient and Directive Generation of Two Distinct Endoderm Lineages from Human ESCs and iPSCs by Differentiation Stage-Specific SOX17 Transduction. PLoS ONE 6(7): e21780. doi:10.1371/journal.pone.0021780

Editor: Patrick Callaerts, VIB & Katholieke Universiteit Leuven, Belgium

Received February 3, 2011; **Accepted** June 8, 2011; **Published** July 7, 2011

Funding: HM, MKF, and TH were supported by grants from the Ministry of Health, Labor, and Welfare of Japan. K. Kawabata was supported by grants from the Ministry of Education, Sports, Science and Technology of Japan (20200076) and the Ministry of Health, Labor, and Welfare of Japan. K. Katayama was supported by the Program for Promotion of Fundamental Studies in Health Sciences of the National Institute of Biomedical Innovation (NIBIO). The funders had no role in study design, data collection and analysis, decision to publish, or preparation of the manuscript.

Competing Interests: The authors have declared that no competing interests exist.

* E-mail: mizuguch@phs.osaka-u.ac.jp

Introduction

There are two distinct endoderm lineages in early embryogenesis, the extraembryonic endoderm (ExEn) and the definitive endoderm (DE). The first of these lineages, the ExEn plays crucial roles in mammalian development, although it does not contribute to the formation of body cells. In early embryogenesis, a part of the inner cell mass of the blastocyst differentiates into the primitive endoderm (PrE). The PrE differentiates into the ExEn that composes the parietal endoderm, which contributes to the primary yolk sac, and the visceral endoderm, which overlies the epiblast [1,2]. In contrast, the second of the endoderm lineages, the DE arises from the primitive streak (PS), which is called the mesendoderm [3]. The DE has the ability to differentiate into the hepatic and pancreatic tissue [4].

The establishment of human embryonic stem cells (ESCs) [5] and human induced pluripotent stem cells (iPSCs) [6,7] has opened up new opportunities for basic research and regenerative medicine. To exploit the potential of human ESCs and iPSCs, it is necessary to understand the mechanisms of their differentiation. Although growth factor-mediated ExEn or DE differentiation is widely performed, it leads to a heterogeneous population [8,9,10,11]. Several studies have utilized not only growth factors but also modulation of transcription factors to control downstream signaling cascades [10,12,13]. Sox17, an Sry-related HMG box transcription factor, is required for development of both the ExEn and DE. In mice, during ExEn and DE development, Sox17 expression is first observed in the PrE and in the anterior PS, respectively [14]. Previous study showed that stable Sox17 overexpression promotes ExEn differentiation from mouse ESCs [12]. On the other hand, another previous study has demonstrated that DE progenitors can be established from human ESCs by stable expression of SOX17 [10]. The mechanism of these discrepancies which occurs in SOX17 transduction still remains unknown. Also, the role of SOX17 in human ExEn differentiation still remains unknown. Therefore, it is quite difficult to promote directive differentiation into either ExEn or DE cells by SOX17 transduction.

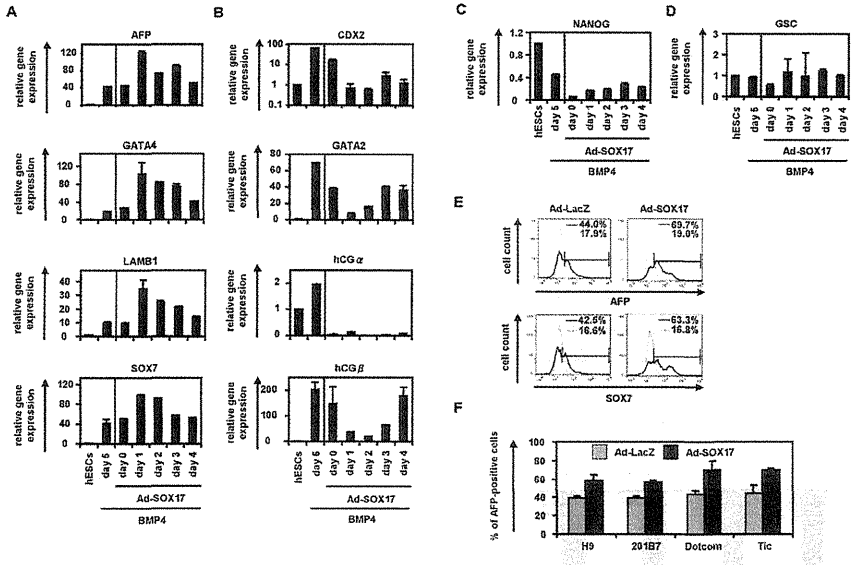

Figure 1. Efficient ExEn differentiation from human ESC- and iPSC-derived PrE cells by SOX17 transduction. (A–D) Undifferentiated human ESCs (H9) and BMP4-induced human ESC-derived cells, which were cultured with the medium containing BMP4 (20 ng/ml) for 0, 1, 2, 3, and 4 days, were transduced with 3,000 VP/cell of Ad-SOX17 for 1.5 h. Ad-SOX17-transduced cells were cultured with 20 ng/ml of BMP4, and then the gene expression levels of *(A)* the ExEn markers (AFP, GATA4, LAMB1, and SOX7), (B) the trophectoderm markers (CDX2, GATA2, hCGα, and hCGβ), (C) the pluripotent marker (NANOG), and (D) the DE marker (GSC) were examined by real-time RT-PCR on day 5 of differentiation. The horizontal axis represents the day on which the cells were transduced with Ad-SOX17. The expression levels of undifferentiated human ESCs on day 0 were defined 1.0. (E) On day 1, human ESC-derived PrE cells, which were cultured with the medium containing BMP4 for 1 day, were transduced with Ad-LacZ or Ad-SOX17 and cultured until day 5. The ExEn cells were subjected to immunostaining with anti-AFP or anti-SOX7 antibodies, and then analyzed by flow cytometry. (F) After Ad-LacZ or Ad-SOX17 transduction, the efficacies of ExEn differentiation from the human ES cell line (H9) and the three human iPS cell lines (201B7, Dotcom, and Tic) were compared on day 5 of differentiation. All data are represented as the means±SD ($n=3$).
doi:10.1371/journal.pone.0021780.g001

In this study, we utilized SOX17 as a stage-specific regulator of ExEn and DE differentiation from human ESCs and iPSCs. The human ESC- and iPSC-derived cells were transduced with SOX17-expressing adenovirus vector (Ad-SOX17), and the resulting phenotypes were assessed for their ability to differentiate into ExEn and DE cells *in vitro*. In addition, we examined whether SOX17-transduced cells have the ability to differentiate into the hepatic lineage. The results showed that stage-specific overexpression of the SOX17 transcription factor promotes directive differentiation into either ExEn or DE cells.

Results

The induction of human ESC-derived PrE cells and human ESC-derived mesendoderm cells

To determine the appropriate stage for SOX17 transduction, ExEn or DE cells were differentiated from human ESCs by a conventional method using BMP4 (20 ng/ml) or Activin A (100 ng/ml), respectively (Figures S1 and S2). Experiments for bidirectional differentiation using BMP4 and Activin A indicated that PrE cells were obtained on day 1 (Figure S1) and mesendoderm cells were obtained on day 3 (Figure S2). We expected that stage-specific SOX17 transduction into PrE cells or mesendoderm cells could promote ExEn or DE differentiation, because the time period of intiation of SOX17 expression was correlated with the time period of formation of PrE cells (day 1) (Figure S1C) and mesendoderm cells (day 3) (Figure S2C), respectively.

PrE stage-specific SOX17 overexpression promotes directive ExEn differentiation from human ESCs

To examine the effect of forced and transient expression of SOX17 on the differentiation of human ESC- and iPSC-derived cells, we used a fiber-modified adenovirus (Ad) vector containing the EF-1α promoter and a stretch of lysine residues (KKKKKKK, K7) peptides in the C-terminal region of the fiber knob. The K7 peptide targets heparan sulfates on the cellular surface, and the fiber-modified Ad vector containing the K7 peptides has been shown to be efficient for transduction into many kinds of cells [15,16].

Because the time period of initiation of SOX17 expression was correlated with the time period of formation of PrE cells (day 1) (Figure S1), we expected that stage-specific SOX17 transduction into PrE cells would promote ExEn differentiation. Therefore, we examined the stage-specific role of SOX17 in ExEn differentiation. Ad-SOX17 transduction was performed in human ESCs treated with BMP4 for 0, 1, 2, 3, or 4 days, and the Ad-SOX17-transduced cells were cultured with medium containing BMP4 until day 5 (Figures 1A–1D). We confirmed the expression of exogenous SOX17 in the human ESC-derived mesendoderm cells transduced with Ad-SOX17 (Figure S3). Since BMP4 is known for its capability to induce both ExEn and trophectoderm [8,9], we analyzed not only the expression levels of ExEn markers but also those of trophectoderm markers by real-time RT-PCR after 5 days of differentiation (Figures 1A and 1B). The transduction of Ad-SOX17 on day 1 led to the highest expression levels of ExEn markers, alpha-fetoprotein (AFP), GATA4, laminin B1 (LAMB1), and SOX7 [17,18,19]. In contrast, the expression levels of the trophectoderm markers CDX2, GATA2, hCGα (human chorionic gonadotropin), and hCGβ [20] were down-regulated in Ad-SOX17-transduced cells as compared with non-transduced cells (Figure 1B). The expression levels of the pluripotent marker NANOG and DE marker GSC were not increased by SOX17 transduction (Figures 1C and 1D). We confirmed that there were no differences between non-transduced cells and Ad-LacZ-transduced cells in gene expression levels of all the markers investigated in Figures 1A–1D (data not shown). Therefore, we concluded that ExEn cells were efficiently induced from Ad-SOX17-transduced PrE cells.

The effects of SOX17 transduction on the ExEn differentiation from human ESC-derived PrE cells were also assessed by quantifying AFP- or SOX7-positive ExEn cells. The percentage of AFP- or SOX7-positive cells was significantly increased in Ad-SOX17-transduced cells (69.7% and 63.3%, respectively) (Figure 1E). Similar results were observed in the human iPS cell lines (201B7, Dotcom, and Tic) (Figure 1F). These findings indicated that stage-specific SOX17 overexpression in human ESC-derived PrE cells enhances ExEn differentiation.

Mesendoderm stage-specific SOX17 overexpression promotes directive DE differentiation from human ESCs

To examine the effects of transient SOX17 overexpression on DE differentiation from human ESCs, we optimized the timing of the Ad-SOX17 transduction. Ad-SOX17 transduction was performed in human ESCs treated with Activin A (100 ng/ml) for 0, 1, 2, 3, or 4 days, and the Ad-SOX17-transduced cells were cultured with medium containing Activin A (100 ng/ml) until day 5 (Figures 2A–2C). Using a fiber-modified Ad vector, both undifferentiated human ESCs and Activin A-induced human ESC-derived cells were efficiently transduced (Figure S4). The transduction of SOX17 on day 3 led to the highest expression levels of the DE markers FOXA2 [21], GSC [22], GATA4 [17], and HEX [23] (Figure 2A). In contrast to the DE markers, the expression levels of the pluripotent marker NANOG [24] were down-regulated in Ad-SOX17-transduced cells as compared with non-transduced cells (Figure 2B). The expression levels of the ExEn marker SOX7 [14] were up-regulated, when Ad-SOX17 transduction was performed into human ESCs treated with Activin A (100 ng/ml) for 0, 1, or 2 days (Figure 2C). On the other hand, the expression levels of the ExEn marker SOX7 were significantly down-regulated, when Ad-SOX17 transduction was performed into human ESCs treated with Activin A (100 ng/ml) for 3 or 4 days, indicating that SOX17 overexpression prior to mesendoderm formation (day 0, 1, and 2) promoted not only DE differentiation but also ExEn differentiation. Similar results were obtained with the human iPS cell line (Tic) (Figure S5). Although the expression levels of the mesoderm marker FLK1 [25] did not exhibit any change when Ad-SOX17 transduction was performed into human ESCs treated with Activin A (100 ng/ml) for 0, 1, or 2 days (Figure 2D), their expression levels were significantly down-regulated when Ad-SOX17 transduction was performed into human ESCs treated with Activin A (100 ng/ml) for 3 or 4 days. These results suggest that SOX17 overexpression promotes directive differentiation from mesendoderm cells into the DE cells, but not into mesoderm cells. We also confirmed that Ad-vector mediated gene expression in the human ESC-derived mesendoderm cells (day 3) continued until day 6 and disappeared on day 10 (Figure S6). SOX17 transduction in the human ESC-derived cells on day 3 and 4 had no effect on cell viability, while that in the cells on day 0, 1, and 2 resulted in severely impaired cell viability (Figure S7), probably because SOX17 transduction directed the cells on day 0, 1, and 2 to differentiate into ExEn cells but the medium containing Activin A (100 ng/ml) was inappropriate for ExEn cells. We confirmed that there were no differences between non-transduced cells and Ad-LacZ-transduced cells in gene expression levels of all the markers investigated in Figures 2A–2D (data not shown). These results indicated that stage-specific SOX17 overexpression in human ESC-derived mesendoderm cells is essential for promoting efficient DE differentiation.

It has been previously reported that human ESC-derived mesendoderm cells and DE cells became CXCR4-positive (>80%) by culturing human ESCs with Activin A (100 ng/ml) [26]. However, Activin A is not sufficient for homogenous differentiation of c-Kit/CXCR4-double-positive DE cells [10,11] or HEX-positive anterior DE cells [23]. Seguin et al. and Morrison et al. reported that the differentiation efficiency of c-Kit/CXCR4-double-positive DE cells was approximately 30% in the absence of stable Sox17 expression and that of HEX-positive anterior DE cells was only about 10% [10,23]. Therefore, we next examined whether Ad-SOX17 transduction improves the differentiation efficiency of c-Kit/CXCR4-double-positive DE cells and HEX-positive anterior DE cells. Human ESC-derived mesendoderm cells were transduced with Ad-SOX17, and the number of CXCR4/c-Kit-double-positive cells was analyzed by using a flow cytometer. The percentage of CXCR4/c-Kit-double-positive cells was significantly increased in Ad-SOX17-transduced cells (67.7%), while that in Ad-LacZ-transduced cells was only 22% (Figure 2E). The percentage of HEX-positive cells was also significantly increased in Ad-SOX17-transduced cells (53.7%), while that in Ad-LacZ-transduced cells was approximately 11% (Figure 2F). Similar results were also observed in the three human iPS cell lines (201B7, Dotcom, and Tic) (Figure 2G). These findings indicated that stage-specific SOX17 overexpression in human ESC-derived mesendoderm cells promotes efficient differentiation of DE cells.

Ad-SOX17-transduced cells tend to differentiate into the hepatic lineage

To investigate whether Ad-SOX17-transduced cells have the ability to differentiate into hepatoblasts and hepatocyte-like cells, Ad-SOX17-transduced cells were differentiated according to our previously described method [13]. Our previous report demonstrated that transient HEX transduction efficiently generates hepatoblasts from human ESC- and iPSC-derived DE cells. The hepatic differentiation protocol used in this study is illustrated in Figure 3A. After the hepatic differentiation, the morphology of human ESCs transduced with Ad-SOX17 followed by Ad-HEX was gradually changed into a hepatocyte morphology: polygonal in shape with distinct round nuclei by day 18 (Figure 3B). We also

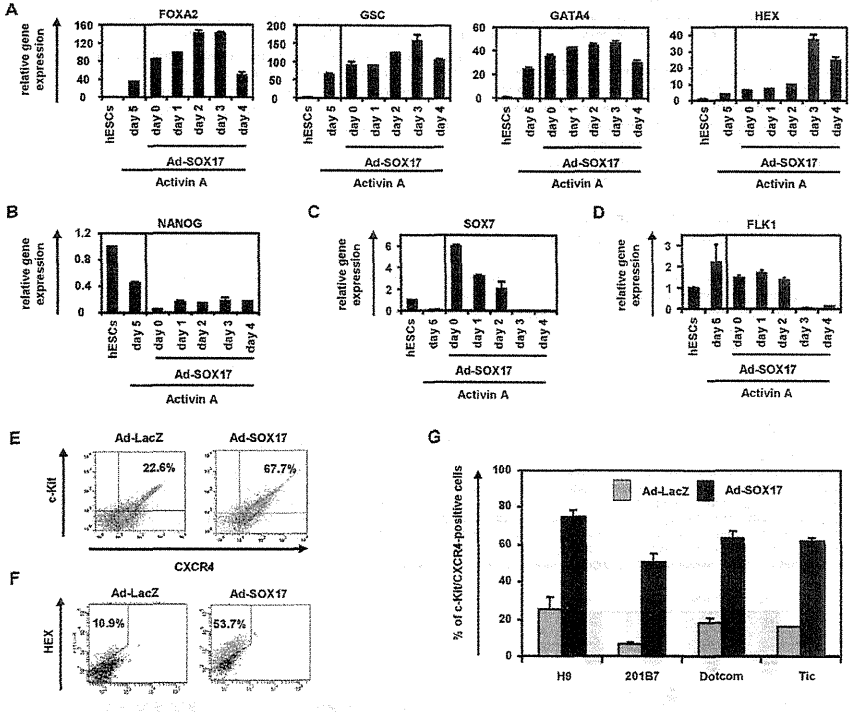

Figure 2. Efficient DE differentiation from human ESC- and iPSC-derived mesendoderm cells by SOX17 transduction. (A–D) Undifferentiated human ESCs (H9) and Activin A-induced human ESC-derived cells, which were cultured with the medium containing Activin A (100 ng/ml) for 0, 1, 2, 3, and 4 days, were transduced with 3,000 VP/cell of Ad-SOX17 for 1.5 h. Ad-SOX17-transduced cells were cultured with 100 ng/ml of Activin A, and the gene expression levels of (A) the DE markers (FOXA2, GSC, and GATA4) and anterior DE marker (HEX), (B) the pluripotent marker (NANOG), (C) the ExEn marker (SOX7), and (D) the mesoderm marker (FLK1) were examined by real-time RT-PCR on day 5 of differentiation. The horizontal axis represents the day on which the cells were transduced with Ad-SOX17. The expression levels of human ESCs on day 0 were defined 1.0. (E, F) After human ESCs were cultured with 100 ng/ml of Activin A for 3 days, human ESC-derived mesendoderm cells were transduced with Ad-LacZ or Ad-SOX17 and cultured until day 5. Ad-LacZ- or Ad-SOX17-transduced DE cells were subjected to immunostaining with anti-c-Kit, anti-CXCR4 (E) and anti-HEX antibodies (F) and then analyzed by flow cytometry. (G) After Ad-LacZ or Ad-SOX17 transduction, the DE differentiation efficacies of the human ES cell line (H9) and three human iPS cell lines (201B7, Dotcom, and Tic) were compared at day 5 of differentiation. All data are represented as the means±SD ($n = 3$).
doi:10.1371/journal.pone.0021780.g002

examined hepatic gene and protein expression levels on day18 of differentiation. For this purpose, we used a human ES cell line (H9) and three human iPS cell lines (201B7, Dotcom, Tic). On day 18 of differentiation, the gene and protein expression analysis showed up-regulation of the hepatic markers albumin (ALB) [27], cytochrome P450 2D6 (CYP2D6), CYP3A4, and CYP7A1 [28] mRNA and ALB, CYP2D6, CYP3A4, CYP7A1, and cytokeratin (CK)18 proteins in both Ad-SOX17- and Ad-HEX-transduced cells transduced cells as compared with both Ad-LacZ- and Ad-HEX-transduced cells (Figures 4A and 4B). These results indicated that Ad-SOX17-transduced cells were more committed to the hepatic lineage than non-transduced cells.

Discussion

The directed differentiation from human ESCs and iPSCs is a useful model system for studying mammalian development as well as a powerful tool for regenerative medicine [29]. In the present study, we elucidated the bidirectional role of SOX17 on either ExEn or DE differentiation from human ESCs and iPSCs. We initially confirmed that initiation of SOX17 expression was consistent with the time period of PrE or mesendoderm cells formation (Figures S1 and S2). We speculated that stage-specific transient SOX17 transduction in PrE or mesendoderm could enhance ExEn or DE differentiation from human ESCs and iPSCs, respectively.

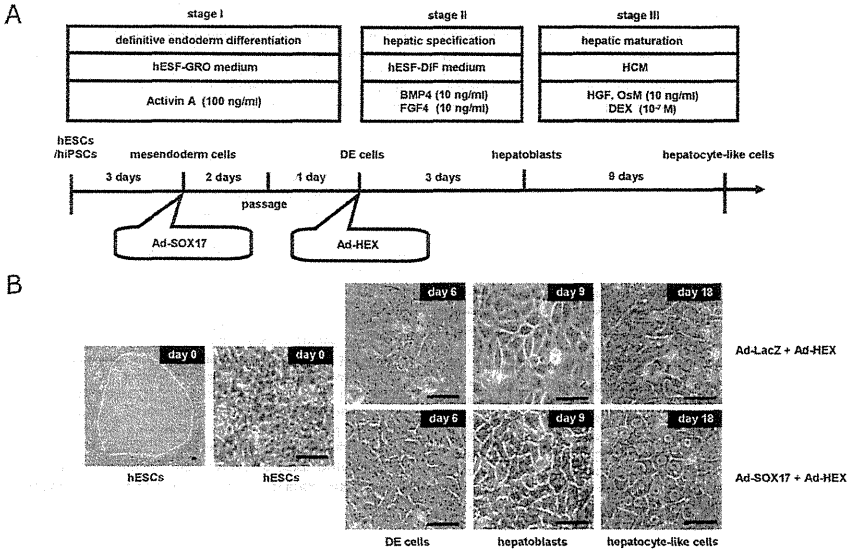

Figure 3. Hepatic Differentiation of Human ESC- and iPSC-Derived DE Cells Transduced with Ad-HEX. (A) The procedure for differentiation of human ESCs and iPSCs into hepatoblasts and hepatocyte-like cells is presented schematically. Both hESF-GRO and hESF-DIF medium were supplemented with 5 factors and 0.5 mg/ml fatty acid-free BSA, as described in the Materials and Methods section. (B) Sequential morphological changes (day 0–18) of human ESCs (H9) differentiated into hepatocyte-like cells via the DE cells and the hepatoblasts are shown. The scale bar represents 50 μm.
doi:10.1371/journal.pone.0021780.g003

SOX17 transduction at the pluripotent stage promoted random differentiation giving heterogeneous populations containing both ExEn and DE cells were obtained (Figures 2A–2C). Qu et al. reported that SOX17 promotes random differentiation of mouse ESCs into PrE cells and DE cells *in vitro* [30], which is in consistent with the present study. Previously, Niakan et al. and Seguin et al. respectively demonstrated that ESCs could promote either ExEn or DE differentiation by stable SOX17 expression, respectively [10,12]. Although these discrepancies might be attributable to differences in the species used in the experiments (i.e., human versus mice), SOX17 might have distinct functions according to the appropriate differentiation stage. To elucidate these discrepancies, we examined the stage-specific roles of SOX17 in the present study, and found that human ESCs and iPSCs could differentiate into either ExEn or DE cells when SOX17 was overexpressed at the PrE or mesendoderm stage, respectively, but not when it was overexpressed at the pluripotent stage (Figures 1 and 2). This is because endogenous SOX17 is strongly expressed in the PrE and primitive streak tissues but only slightly expressed in the inner cell mass, our system might adequately reflect the early embryogenesis [14,31].

In ExEn differentiation from human ESCs, stage-specific SOX17 overexpression in human ESC-derived PrE cells promoted efficient ExEn differentiation and repressed trophectoderm differentiation (Figures 1A and 1B), although SOX17 transduction at the pluripotent stage did not induce the efficient differentiation of ExEn cells. In our protocol, the stage-specific overexpression of SOX17 could elevate the efficacy of AFP-positive or SOX7-positive ExEn differentiation from human ESCs and iPSCs. The reason for the efficient ExEn differentiation by SOX17 transduction might be due to the fact that SOX17 lies downstream from GATA6 and directly regulates the expression of GATA4 and GATA6 [12]. Although it was previously been reported that Sox17 plays a substantial role in late-stage differentiation of ExEn cells *in vitro* [32], those reports utilized embryoid body formation, in which other types of cells, including endoderm, mesoderm, and ectoderm cells, might have influences on cellular differentiation. The present study showed the role of SOX17 in a homogeneous differentiation system by utilizing a mono-layer culture system.

In DE differentiation from human ESCs, we found that DE cells were efficiently differentiated from the human ESC-derived mesendoderm cells by stage-specific SOX17 overexpression (Figure 2). Therefore, we concluded that SOX17 plays a significant role in the differentiation of mesendoderm cells to DE cells. Although SOX17 overexpression before the formation of mesendoderm cells did not affect mesoderm differentiation, SOX17 transduction at the mesendoderm stage selectively promoted DE differentiation and repressed mesoderm differentiation (Figures 2A and 2D). These results show that SOX17 plays a crucial role in decision of DE differentiation from mesendoderm cells, as previous studies suggested [33,34]. Interestingly, SOX17 transduction at the pluripotent stage promoted not only DE

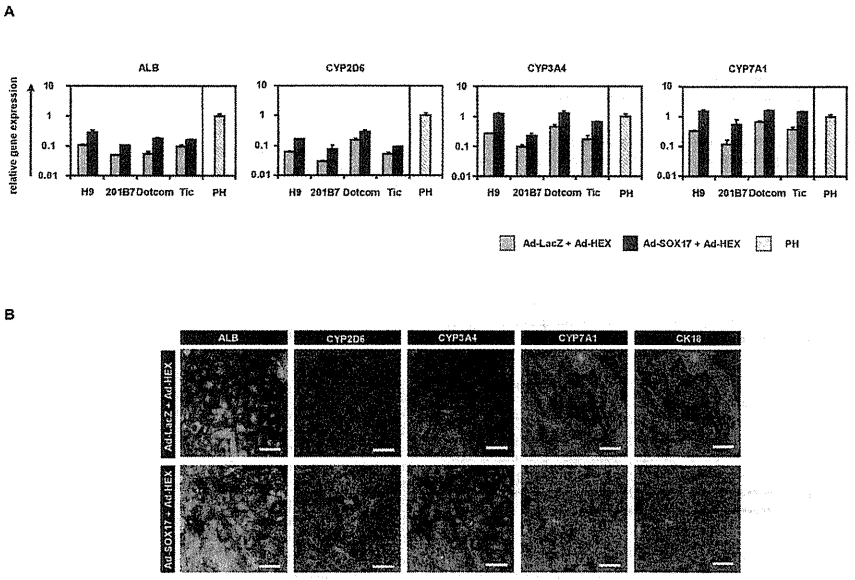

Figure 4. Characterization of hepatocyte-like cells from human ESC- and iPSC-derived DE cells. (A) The Ad-LacZ-transduced cells and Ad-SOX17-transduced cells were transduced with 3,000 VP/cell of Ad-HEX for 1.5 h on day 6. On day 18 of differentiation, the levels of expression of the hepatocyte markers (ALB, CYP2D6, CYP3A4, and CYP7A1) were examined by real-time RT-PCR in human ESC (H9)-derived hepatocyte-like cells and human iPSC (201B7, Dotcom, or Tic)-derived hepatocyte-like cells. The gene expression profiles of cells transduced with both Ad-SOX17 and Ad-HEX (black bar) were compared with those of cells transduced with both Ad-LacZ and Ad-HEX (gray bar). The expression level of primary human hepatocytes (PH, hatched bar), which were cultured 48 h after plating the cells, were defined as 1.0. All data are represented as the means±SD ($n = 3$). (B) The expression of the hepatocyte markers ALB (green), CYP2D6 (red), CYP3A4 (red), CYP7A1 (red), and CK18 (green) was also examined by immunohistochemistry on day 18 of differentiation. Nuclei were counterstained with DAPI (blue). The scale bar represents 50 μm.
doi:10.1371/journal.pone.0021780.g004

differentiation but also ExEn differentiation even in the presence of Activin A (Figures 2A and 2C), demonstrating that transduction at an inappropriate stage of differentiation prevents directed differentiation. These results suggest that stage-specific SOX17 transduction mimicking the gene expression pattern in embryogenesis could selectively promote DE differentiation.

Another important finding about DE differentiation is that the protocol in the present study was sufficient for nearly homogeneous DE and anterior DE differentiation by mesendoderm stage-specific SOX17 overexpression; the differentiation efficacies of c-Kit/CXCR4-double-positive DE cells and HEX-positive anterior DE cells were approximately 70% and 54%, respectively (Figures 2E and 2F). The conventional differentiation protocols without gene transfer were not sufficient for homogenous DE and anterior DE differentiation; the differentiation efficacies of DE and anterior DE were approximately 30% and 10%, respectively [10,11,23]. One of the reasons for the efficient DE differentiation by SOX17 transduction might be the activation of the FOXA2 gene which could regulate many endoderm-associated genes [35]. Moreover, SOX17-transduced cells were more committed to the hepatic lineage (Figure 4). This might be because the number of HEX-positive anterior DE cell populations was increased by SOX17 transduction. Recent studies have shown that the conditional expression of Sox17 in the pancreas at E12.5, when it is not normally expressed, is sufficient to promote biliary differentiation at the expense of endocrine cells [36]. Therefore, we reconfirmed that our protocol in which SOX17 was transiently transduced at the appropriate stage of differentiation was useful for DE and hepatic differentiation from human ESCs and iPSCs.

Using human iPSCs as well as human ESCs, we confirmed that stage-specific overexpression of SOX17 could promote directive differentiation of either ExEn or DE cells (Figures 1F, 2G, and 4A). Interestingly, a difference of DE and hepatic differentiation efficacy among human iPS cell lines was observed (Figures 1F and 2G). Therefore, it would be necessary to select a human iPS cell line that is suitable for hepatic differentiation in the case of medical applications, such as liver transplantation.

To control cellular differentiation mimicking embryogenesis, we employed Ad vectors, which are one of the most efficient transient gene delivery vehicles and have been widely used in both experimental studies and clinical trials [37]. Recently, we have also demonstrated that ectopic HEX expression by Ad vectors in human ESC-derived DE cells markedly enhances the hepatic differentiation [13]. Thus, Ad vector-mediated transient gene transfer should be a powerful tool for regulating cellular differentiation.

In summary, the findings presented here demonstrate a stage-specific role of SOX17 in the ExEn and DE differentiation from human ESCs and iPSCs (Figure S8). Although previous reports showed that SOX17 overexpression in ESCs leads to differentiation of either ExEn or DE cells, we established a novel method to promote directive differentiation by SOX17 transduction. Because we utilized a stage-specific overexpression system, our findings provide further evidence that the lineage commitment in this method seems to reflects what is observed in embryonic development. In the present study, both human ESCs and iPSCs (3 lines) were used and all cell lines showed efficient ExEn or DE differentiation, indicating that our novel protocol is a powerful tool for efficient and cell line-independent endoderm differentiation. Moreover, the establishing methods for efficient hepatic differentiation by sequential SOX17 and HEX transduction would be useful for *in vitro* applications such as screening of pharmacological compounds as well as for regenerative therapy.

Materials and Methods

In vitro Differentiation

Before the initiation of cellular differentiation, the medium of human ESCs and iPSCs was exchanged for a defined serum-free medium hESF9 [38] and cultured as we previously reported. hESF9 consists of hESF-GRO medium (Cell Science & Technology Institute) supplemented with 5 factors (10 μg/ml human recombinant insulin, 5 μg/ml human apotransferrin, 10 μM 2-mercaptoethanol, 10 μM ethanolamine, and 10 μM sodium selenite), oleic acid conjugated with fatty acid free bovine albumin, 10 ng/ml FGF2, and 100 ng/ml heparin (all from Sigma).

To induce, ExEn cells, human ESCs and iPSCs were cultured for 5 days on a gelatin-coated plate in mouse embryonic conditioned-medium supplemented with 20 ng/ml BMP4 (R&D system) and 1% FCS (GIBCO-BRL).

The differentiation protocol for induction of DE cells, hepatoblasts, and hepatocyte-like cells was based on our previous report with some modifications [13]. Briefly, in DE differentiation, human ESCs and iPSCs were cultured for 5 days on a Matrigel (BD)-coated plate in hESF-DIF medium (Cell Science & Technology Institute) supplemented with the above-described 5 factors, 0.5 mg/ml BSA, and 100 ng/ml Activin A (R&D Systems). For induction of hepatoblasts, the DE cells were transduced with 3,000 VP/cell of Ad-HEX for 1.5 h and cultured in hESF-DIF (Cell Science & Technology Institute) medium supplemented with the above-described 5 factors, 0.5 mg/ml BSA, 10 ng/ml bone morphology protein 4 (BMP4) (R&D Systems), and 10 ng/ml FGF4 (R&D systems). In hepatic differentiation, the cells were cultured in hepatocyte culture medium (HCM) supplemented with SingleQuots (Lonza), 10 ng/ml hepatocyte growth factor (HGF) (R&D Systems), 10 ng/ml Oncostatin M (OsM) (R&D Systems), and 10^{-7} M dexamethasone (DEX) (Sigma).

Human ESC and iPSC Culture

A human ES cell line, H9 (WiCell Research Institute), was maintained on a feeder layer of mitomycin C-treated mouse embryonic fibroblasts (Millipore) with Repro Stem (Repro CELL), supplemented with 5 ng/ml fibroblast growth factor 2 (FGF2) (Sigma). Human ESCs were dissociated with 0.1 mg/ml dispase (Roche Diagnostics) into small clumps, and subcultured every 4 or 5 days. Two human iPS cell lines generated from the human embryonic lung fibroblast cell line MCR5 were provided from the JCRB Cell Bank (Tic, JCRB Number: JCRB1331; and Dotcom, JCRB Number: JCRB1327) [39,40]. These human iPS cell lines were maintained on a feeder layer of mitomycin C-treated mouse embryonic fibroblasts with iPSellon (Cardio), supplemented with 10 ng /ml FGF2. Another human iPS cell line, 201B7, generated from human dermal fibroblasts (HDF) was kindly provided by Dr. S. Yamanaka (Kyoto University) [6]. The human iPS cell line 201B7 was maintained on a feeder layer of mitomycin C-treated mouse embryonic fibroblasts with Repro Stem (Repro CELL), supplemented with 5 ng/ml FGF2 (Sigma). Human iPSCs were dissociated with 0.1 mg/ml dispase (Roche Diagnostics) into small clumps, and subcultured every 5 or 6 days.

Adenovirus (Ad) Vectors

Ad vectors were constructed by an improved *in vitro* ligation method [41,42]. The human SOX17 gene (accession number NM_022454) was amplified by PCR using primers designed to incorporate the 5′ BamHI and 3′ XbaI restriction enzyme sites: Fwd 5′-gcagggatccagcgccatgagcagccggg-3′ and Rev 5′-cttctagagatcagggacctgtcacacgtc-3′. The human SOX17 gene was inserted into pcDNA3 (Invitrogen), resulting in pcDNA-SOX17, and then the human SOX17 gene was inserted into pHMEF5 [15], which contains the human EF-1α promoter, resulting in pHMEF-SOX17. The pHMEF-SOX17 was digested with I-CeuI/PI-SceI and ligated into I-CeuI/PI-SceI-digested pAdHM41-K7 [16], resulting in pAd-SOX17. The human elongation factor-1α (EF-1α) promoter-driven LacZ- or HEX-expressing Ad vectors, Ad-LacZ or Ad-HEX, were constructed previously. [13,43]. Ad-SOX17, Ad-HEX, and Ad-LacZ, which contain a stretch of lysine residue (K7) peptides in the C-terminal region of the fiber knob for more efficient transduction of human ESCs, iPSCs, and DE cells, were generated and purified as described previously [13,15,43]. The vector particle (VP) titer was determined by using a spectrophotometric method [44].

Flow Cytometry

Single-cell suspensions of human ESCs, iPSCs, and their derivatives were fixed with methanol at 4°C for 20 min, then incubated with the primary antibody, followed by the secondary antibody. Flow cytometry analysis was performed using a FACS LSR Fortessa flow cytometer (Becton Dickinson).

RNA Isolation and Reverse Transcription-Polymerase Chain Reaction (RT-PCR)

Total RNA was isolated from human ESCs, iPSCs, and their derivatives using ISOGENE (Nippon Gene) according to the manufacture's instructions. Primary human hepatocytes were purchased from CellzDirect. cDNA was synthesized using 500 ng of total RNA with a Superscript VILO cDNA synthesis kit (Invitrogen). Real-time RT-PCR was performed with Taqman gene expression assays (Applied Biosystems) or SYBR Premix Ex Taq (TaKaRa) using an ABI PRISM 7000 Sequence Detector (Applied Biosystems). Relative quantification was performed against a standard curve and the values were normalized against the input determined for the housekeeping gene, glyceraldehyde 3-phosphate dehydrogenase (GAPDH). The primer sequences used in this study are described in Table S1.

Immunohistochemistry

The cells were fixed with methanol or 4% PFA. After blocking with PBS containing 2% BSA and 0.2% Triton X-100 (Sigma), the cells were incubated with primary antibody at 4°C for 16 h, followed by incubation with a secondary antibody that was labeled

with Alexa Fluor 488 or Alexa Fluor 594 (Invitrogen) at room temperature for 1 h. All the antibodies are listed in Table S2.

Crystal Violet Staining

The human ESC-derived cells that had adhered to the wells were stained with 200 µl of 0.3% crystal violet solution at room temperature for 15 min. Excess crystal violet was then removed and the wells were washed three times. Fixed crystal violet was solubilized in 200 µl of 100% ethanol at room temperature for 15 min. Cell viability was estimated by measuring the absorbance at 595 nm of each well using a microtiter plate reader (Sunrise, Tecan).

LacZ Assay

The human ESC- and iPSC-derived cells were transduced with Ad-LacZ at 3,000 VP/cell for 1.5 h. After culturing for the indicated number of days, 5-bromo-4-chloro-3-indolyl β-D-galactopyranoside (X-Gal) staining was performed as described previously [15].

Supporting Information

Table S1 List of Taqman probes and primers used in this study.
(DOC)

Table S2 List of antibodies used in this study.
(DOC)

Figure S1 PrE cells formation from human ESCs on day 1 of differentiation. (A) The procedure for differentiation of human ESCs and iPSCs to ExEn cells by treatment with BMP4 (20 ng/ml) is presented schematically. (B) Human ESCs (H9) were morphologically changed during ExEn differentiation; when human ESCs were cultured with the medium containing BMP4 (20 ng/ml) for 5 days, the cells began to show flattened epithelial morphology. The scale bar represents 50 µm. (C–E) The tTemporal protein expression analysis during ExEn differentiation was performed by immunohistochemistry. The PrE markers COUP-TF1 [21] (red), SOX17 [14] (red), and SOX7 [14] (red) were detected on day 1. In contrast to the PS markers, the expression of the DE marker GSC [22] (red) was not detected and the level of the pluripotent marker NANOG (green) declined between day 0 and day 1. Nuclei were counterstained with DAPI (blue). The scale bar represents 50 µm.
(PDF)

Figure S2 Mesendoderm cells formation from human ESCs on day 3 of differentiation. (A) The procedure for differentiation of human ESCs and iPSCs to DE cells by treatment with Activin A (100 ng/ml) is presented schematically. hESF-GRO medium was supplemented with 5 factors and 0.5 mg/ml fatty acid free BSA, as described in the Materials and Methods. (B) Human ESCs (H9) were morphologically changed during DE differentiation; when human ESCs were cultured with the medium containing Activin A (100 ng/ml) for 5 days, the morphology of the cells began to show visible cell-cell boundaries. The scale bar represents 50 µm. (C–E) The tTemporal protein expression analysis during DE differentiation was performed by immunohistochemistry. The anterior PS markers FOXA2 [21] (red), GSC [22] (red), and SOX17 [14] (red) were adequately detected on day 3. The PS marker T [45] (red) was detected until day 3. In contrast to the PS markers, the expression of the pluripotent marker NANOG [24] (green) declined between day 2 and day 3. Nuclei were counterstained with DAPI (blue). The scale bar represents 50 µm.
(PDF)

Figure S3 Overexpression of SOX17 mRNA in human ESC (H9)-derived PS cells by Ad-SOX17 transduction. Human ESC-derived PS cells (day 1) were transduced with 3,000VP/cell of Ad-SOX17 for 1.5 h. On day 3 of differentiation, real-time RT-PCR analysis of the SOX17 expression was performed in Ad-LacZ-transduced cells and Ad-SOX17-transduced cells. On the y axis, the expression levels of undifferentiated human ESCs on day 0 was were taken defined as 1.0. All data are represented as the means±SD ($n = 3$).
(PDF)

Figure S4 Efficient transduction in Activin A-induced human ESC (H9)-derived cells by using a fiber-modified Ad vector containing the EF-1α promoter. Undifferentiated human ESCs and Activin A-induced human ESC-derived cells, which were cultured with the medium containing Activin A (100 ng/ml) for 0, 1, 2, 3, and 4 days, were transduced with 3,000 vector particles (VP)/cell of Ad-LacZ for 1.5 h. The day after transduction, X-gal staining was performed. The scale bar represents 100 µm. Similar results were obtained in two independent experiments.
(PDF)

Figure S5 Optimization of the time period for Ad-SOX17 transduction to promote DE differentiation from human iPSCs (Tic). Undifferentiated human iPSCs and Activin A-induced human iPSC-derived cells, which were cultured with the medium containing Activin A (100 ng/ml) for 0, 1, 2, 3, and 4 days, were transduced with 3,000 VP/cell of Ad-SOX17 for 1.5 h. Ad-SOX17-transduced cells were cultured with Activin A (100 ng/ml) until day 5, and then real-time RT-PCR analysis was performed. The horizontal axis represents the day on which the cells were transduced with Ad-SOX17. On the y axis, the expression levels of undifferentiated cells on day 0 was were taken defined as 1.0. All data are represented as the means±SD ($n = 3$).
(PDF)

Figure S6 Time course of LacZ expression in human ESC (H9)-derived mesendoderm cells transduced with Ad-LacZ. The hHuman ESC-derived mesendoderm cells (day 3) were transduced with 3,000 VP/cell of Ad-LacZ for 1.5 h. On days 4, 5, 6, 8, and 10, X-gal staining was performed. Note that human ESC-derived cells were passaged on day 5. The scale bar represents 100 µm. Similar results were obtained in two independent experiments.
(PDF)

Figure S7 Optimization of the time period for Ad-SOX17 transduction into Activin A-induced human ESC (H9)-derived cells. Undifferentiated human ESCs and Activin A-induced hESC-derived cells, which were cultured with the medium containing Activin A (100 ng/ml) for 0, 1, 2, 3, and 4 days, were transduced with 3,000 VP/cell of Ad-LacZ or Ad-SOX17 for 1.5 h. Ad-SOX17-transduced cells were cultured with Activin A (100 ng/ml) until day 5, then the cell viability was evaluated with crystal violet staining. The horizontal axis represents the day on which the cells were transduced with Ad-SOX17. On the y axis, the level of non-transduced cells was taken defined as 1.0. All data are represented as the means±SD (n = 3).
(PDF)

Figure S8 Model of differentiation of human ESCs and iPSCs into ExEn and DE cells by stage-specific SOX17 transduction. The ExEn and DE differentiation process is divided into at least two stages. In the first stage, human ESCs differentiate into either PrE cells by treatment with BMP4 (20 ng/ml) or mesendoderm cells by treatment with Activin A (100 ng/ml). In the second stage, SOX17 promotes the further differentiation of each precursor cell into ExEn and DE cells, respectively. We have demonstrated that the efficient differentiation of these two distinct endoderm lineages is accomplished by stage-specific SOX17 transduction.
(PDF)

Acknowledgments

We thank Hiroko Matsumura and Misae Nishijima for their excellent technical support. We thank Mr. David Bennett and Ms. Ong Tyng Tyng for critical reading of the manuscript.

References

1. Enders AC, Given RL, Schlafke S (1978) Differentiation and migration of endoderm in the rat and mouse at implantation. Anat Rec 190: 65–77.
2. Gardner RL (1983) Origin and differentiation of extraembryonic tissues in the mouse. Int Rev Exp Pathol 24: 63–133.
3. Grapin-Botton A, Constam D (2007) Evolution of the mechanisms and molecular control of endoderm formation. Mech Dev 124: 253–278.
4. Tam PP, Kanai-Azuma M, Kanai Y (2003) Early endoderm development in vertebrates: lineage differentiation and morphogenetic function. Curr Opin Genet Dev 13: 393–400.
5. Thomson JA, Itskovitz-Eldor J, Shapiro SS, Waknitz MA, Swiergiel JJ, et al. (1998) Embryonic stem cell lines derived from human blastocysts. Science 282: 1145–1147.
6. Takahashi K, Tanabe K, Ohnuki M, Narita M, Ichisaka T, et al. (2007) Induction of pluripotent stem cells from adult human fibroblasts by defined factors. Cell 131: 861–872.
7. Yu J, Vodyanik MA, Smuga-Otto K, Antosiewicz-Bourget J, Frane JL, et al. (2007) Induced pluripotent stem cell lines derived from human somatic cells. Science 318: 1917–1920.
8. Xu RH, Chen X, Li DS, Li R, Addicks GC, et al. (2002) BMP4 initiates human embryonic stem cell differentiation to trophoblast. Nat Biotechnol 20: 1261–1264.
9. Pera MF, Andrade J, Houssami S, Reubinoff B, Trounson A, et al. (2004) Regulation of human embryonic stem cell differentiation by BMP-2 and its antagonist noggin. J Cell Sci 117: 1269–1280.
10. Seguin CA, Draper JS, Nagy A, Rossant J (2008) Establishment of endoderm progenitors by SOX transcription factor expression in human embryonic stem cells. Cell Stem Cell 3: 182–195.
11. Gouon-Evans V, Boussemart L, Gadue P, Nierhoff D, Koehler CI, et al. (2006) BMP-4 is required for hepatic specification of mouse embryonic stem cell-derived definitive endoderm. Nat Biotechnol 24: 1402–1411.
12. Niakan KK, Ji H, Maehr R, Vokes SA, Rodolfa KT, et al. (2010) Sox17 promotes differentiation in mouse embryonic stem cells by directly regulating extraembryonic gene expression and indirectly antagonizing self-renewal. Genes Dev 24: 312–326.
13. Inamura M, Kawabata K, Takayama K, Tashiro K, Sakurai F, et al. (2011) Efficient Generation of Hepatoblasts From Human ES Cells and iPS Cells by Transient Overexpression of Homeobox Gene HEX. Mol Ther 19: 400–407.
14. Kanai-Azuma M, Kanai Y, Gad JM, Tajima Y, Taya C, et al. (2002) Depletion of definitive gut endoderm in Sox17-null mutant mice. Development 129: 2367–2379.
15. Kawabata K, Sakurai F, Yamaguchi T, Hayakawa T, Mizuguchi H (2005) Efficient gene transfer into mouse embryonic stem cells with adenovirus vectors. Mol Ther 12: 547–554.
16. Koizumi N, Mizuguchi H, Utoguchi N, Watanabe Y, Hayakawa T (2003) Generation of fiber-modified adenovirus vectors containing heterologous peptides in both the HI loop and C terminus of the fiber knob. J Gene Med 5: 267–276.
17. Fujikura J, Yamato E, Yonemura S, Hosoda K, Masui S, et al. (2002) Differentiation of embryonic stem cells is induced by GATA factors. Genes Dev 16: 784–789.
18. Koutsourakis M, Langeveld A, Patient R, Beddington R, Grosveld F (1999) The transcription factor GATA6 is essential for early extraembryonic development. Development 126: 723–732.
19. Morrisey EE, Tang Z, Sigrist K, Lu MM, Jiang F, et al. (1998) GATA6 regulates HNF4 and is required for differentiation of visceral endoderm in the mouse embryo. Genes Dev 12: 3579–3590.
20. Kunath T, Strumpf D, Rossant J (2004) Early trophoblast determination and stem cell maintenance in the mouse–a review. Placenta 25 Suppl A: S32–38.
21. Sasaki H, Hogan BL (1993) Differential expression of multiple fork head related genes during gastrulation and axial pattern formation in the mouse embryo. Development 118: 47–59.
22. Blum M, Gaunt SJ, Cho KW, Steinbeisser H, Blumberg B, et al. (1992) Gastrulation in the mouse: the role of the homeobox gene goosecoid. Cell 69: 1097–1106.
23. Morrison GM, Oikonomopoulou I, Migueles RP, Soneji S, Livigni A, et al. (2008) Anterior definitive endoderm from ESCs reveals a role for FGF signaling. Cell Stem Cell 3: 402–415.
24. Mitsui K, Tokuzawa Y, Itoh H, Segawa K, Murakami M, et al. (2003) The homeoprotein Nanog is required for maintenance of pluripotency in mouse epiblast and ES cells. Cell 113: 631–642.
25. Shalaby F, Rossant J, Yamaguchi TP, Gertsenstein M, Wu XF, et al. (1995) Failure of blood-island formation and vasculogenesis in Flk-1-deficient mice. Nature 376: 62–66.
26. D'Amour KA, Agulnick AD, Eliazer S, Kelly OG, Kroon E, et al. (2005) Efficient differentiation of human embryonic stem cells to definitive endoderm. Nat Biotechnol 23: 1534–1541.
27. Shiojiri N (1984) The origin of intrahepatic bile duct cells in the mouse. J Embryol Exp Morphol 79: 25–39.
28. Ingelman-Sundberg M, Oscarson M, McLellan RA (1999) Polymorphic human cytochrome P450 enzymes: an opportunity for individualized drug treatment. Trends Pharmacol Sci 20: 342–349.
29. Murry CE, Keller G (2008) Differentiation of embryonic stem cells to clinically relevant populations: lessons from embryonic development. Cell 132: 661–680.
30. Qu XB, Pan J, Zhang C, Huang SY (2008) Sox17 facilitates the differentiation of mouse embryonic stem cells into primitive and definitive endoderm in vitro. Dev Growth Differ 50: 585–593.
31. Sherwood RI, Jitianu C, Cleaver O, Shaywitz DA, Lamenzo JO, et al. (2007) Prospective isolation and global gene expression analysis of definitive and visceral endoderm. Dev Biol 304: 541–555.
32. Shimoda M, Kanai-Azuma M, Hara K, Miyazaki S, Kanai Y, et al. (2007) Sox17 plays a substantial role in late-stage differentiation of the extraembryonic endoderm in vitro. J Cell Sci 120: 3859–3869.
33. Yasunaga M, Tada S, Torikai-Nishikawa S, Nakano Y, Okada M, et al. (2005) Induction and monitoring of definitive and visceral endoderm differentiation of mouse ES cells. Nat Biotechnol 23: 1542–1550.
34. Gadue P, Huber TL, Paddison PJ, Keller GM (2006) Wnt and TGF-beta signaling are required for the induction of an in vitro model of primitive streak formation using embryonic stem cells. Proc Natl Acad Sci U S A 103: 16806–16811.
35. Levinson-Dushnik M, Benvenisty N (1997) Involvement of hepatocyte nuclear factor 3 in endoderm differentiation of embryonic stem cells. Mol Cell Biol 17: 3817–3822.
36. Spence JR, Lange AW, Lin SC, Kaestner KH, Lowy AM, et al. (2009) Sox17 regulates organ lineage segregation of ventral foregut progenitor cells. Dev Cell 17: 62–74.
37. Mizuguchi H, Hayakawa T (2004) Targeted adenovirus vectors. Hum Gene Ther 15: 1034–1044.
38. Furue MK, Na J, Jackson JP, Okamoto T, Jones M, et al. (2008) Heparin promotes the growth of human embryonic stem cells in a defined serum-free medium. Proc Natl Acad Sci U S A 105: 13409–13414.
39. Makino H, Toyoda M, Matsumoto K, Saito H, Nishino K, et al. (2009) Mesenchymal to embryonic incomplete transition of human cells by chimeric OCT4/3 (POU5F1) with physiological co-activator EWS. Exp Cell Res 315: 2727–2740.
40. Nagata S, Toyoda M, Yamaguchi S, Hirano K, Makino H, et al. (2009) Efficient reprogramming of human and mouse primary extra-embryonic cells to pluripotent stem cells. Genes Cells 14: 1395–1404.
41. Mizuguchi H, Kay MA (1998) Efficient construction of a recombinant adenovirus vector by an improved in vitro ligation method. Hum Gene Ther 9: 2577–2583.
42. Mizuguchi H, Kay MA (1999) A simple method for constructing E1- and E1/E4-deleted recombinant adenoviral vectors. Hum Gene Ther 10: 2013–2017.
43. Tashiro K, Kawabata K, Sakurai H, Kurachi S, Sakurai F, et al. (2008) Efficient adenovirus vector-mediated PPAR gamma gene transfer into mouse embryoid bodies promotes adipocyte differentiation. J Gene Med 10: 498–507.
44. Maizel JV, Jr., White DO, Scharff MD (1968) The polypeptides of adenovirus. I. Evidence for multiple protein components in the virion and a comparison of types 2, 7A, and 12. Virology 36: 115–125.
45. Wilkinson DG, Bhatt S, Herrmann BG (1990) Expression pattern of the mouse T gene and its role in mesoderm formation. Nature 343: 657–659.

Author Contributions

Conceived and designed the experiments: K. Takayama MI K. Kawabata MFK HM. Performed the experiments: K. Takayama MI K. Tashiro. Analyzed the data: K. Takayama MI K. Kawabata K. Tashiro K. Katayama FS HM. Contributed reagents/materials/analysis tools: K. Kawabata K. Katayama FS TH MFK HM. Wrote the paper: K. Takayama K. Kawabata HM.

Stem Cell Research (2012) 8, 300–311

Available online at www.sciencedirect.com

SciVerse ScienceDirect

www.elsevier.com/locate/scr

SHORT REPORT

Promotion of hematopoietic differentiation from mouse induced pluripotent stem cells by transient HoxB4 transduction

Katsuhisa Tashiro [a], Kenji Kawabata [a,b], Miyuki Omori [a,b], Tomoko Yamaguchi [a], Fuminori Sakurai [b], Kazufumi Katayama [b], Takao Hayakawa [c,d], Hiroyuki Mizuguchi [a,b,e,*]

[a] *Laboratory of Stem Cell Regulation, National Institute of Biomedical Innovation, 7-6-8, Saito-Asagi, Ibaraki, Osaka 567-0085, Japan*
[b] *Graduate School of Pharmaceutical Sciences, Osaka University, 1-6, Yamadaoka, Suita, Osaka, 565-0871, Japan*
[c] *Pharmaceutics and Medical Devices Agency, 3-3-2, Kasumigaseki, Chiyoda-Ku, Tokyo 100-0013, Japan*
[d] *Pharmaceutical Research and Technology Institute, Kinki University, 3-4-1, Kowakae, Higashi-Osaka, Osaka 577-8502, Japan*
[e] *The Center for Advanced Medical Engineering and Informatics, Osaka University, 1-6, Yamadaoka, Suita, Osaka, 565-0871, Japan*

Received 25 April 2011; received in revised form 1 September 2011; accepted 5 September 2011
Available online 16 September 2011

Abstract Ectopic expression of HoxB4 in embryonic stem (ES) cells leads to an efficient production of hematopoietic cells, including hematopoietic stem/progenitor cells. Previous studies have utilized a constitutive HoxB4 expression system or tetracycline-regulated HoxB4 expression system to induce hematopoietic cells from ES cells. However, these methods cannot be applied therapeutically due to the risk of transgenes being integrated into the host genome. Here, we report the promotion of hematopoietic differentiation from mouse ES cells and induced pluripotent stem (iPS) cells by transient HoxB4 expression using an adenovirus (Ad) vector. Ad vector could mediate efficient HoxB4 expression in ES cell-derived embryoid bodies (ES-EBs) and iPS-EBs, and its expression was decreased during cultivation, showing that Ad vector transduction was transient. A colony-forming assay revealed that the number of hematopoietic progenitor cells with colony-forming potential in HoxB4-transduced cells was significantly increased in comparison with that in non-transduced cells or LacZ-transduced cells. HoxB4-transduced cells also showed more efficient generation of CD41-, CD45-, or Sca-1-positive cells than control cells. These results indicate that transient, but not constitutive, HoxB4 expression is sufficient to augment the hematopoietic differentiation of ES and iPS cells, and that our method would be useful for clinical applications, such as cell transplantation therapy.

* Corresponding author at: Laboratory of Biochemistry and Molecular Biology, Graduate School of Pharmaceutical Sciences, Osaka University, 1-6 Yamadaoka, Suita, Osaka 565-0871, Japan. Fax: +81 6 6879 8186.
E-mail address: mizuguch@phs.osaka-u.ac.jp (H. Mizuguchi).

1873-5061/$ - see front matter © 2011 Elsevier B.V. All rights reserved.
doi:10.1016/j.scr.2011.09.001

Introduction

Embryonic stem (ES) cells and induced pluripotent stem (iPS) cells, each of which is derived from the inner cell mass of blastocysts and somatic cells by transducing three or four transcription factors, respectively, can differentiate into various types of cells *in vitro*. They are thus considered as a valuable model to understand the processes involved in the differentiation of lineage-committed cells as well as an unlimited source of cells for therapeutic applications such as hematopoietic stem/progenitor cell (HSPC) transplantation (Evans and Kaufman, 1981; Thomson et al., 1998; Keller, 2005; Takahashi and Yamanaka, 2006; Takahashi et al., 2007).

Differentiation of ES and iPS cells into mature hematopoietic cells, including erythrocytes, myeloid cells, and lymphoid cells, has been performed by embryoid body (EB) formation or coculture with stromal cells (Nakano et al., 1994; Chadwick et al., 2003; Schmitt et al., 2004; Vodyanik et al., 2005). However, the development of an efficient differentiation method for immature hematopoietic cells, including HSPCs, from ES and iPS cells has been challenging. Previously, Daley and his colleagues have shown that enforced expression of HoxB4 in mouse ES cells by a retrovirus vector robustly enhanced the differentiation of ES cells into HSPCs *in vitro*, and these ES cell-derived HSPCs had a long-term reconstitution potential *in vivo* (Kyba et al., 2002; Wang et al., 2005). In addition, constitutive expression of HoxB4 was shown to induce the hematopoietic differentiation from human ES cells (Bowles et al., 2006). These findings indicated that manipulation of HoxB4 expression would be effective for production of HSPCs from ES and iPS cells. However, it is known that long-term constitutive HoxB4 expression in HSPCs has an inhibitory effect on the differentiation of certain hematopoietic lineages, such as lymphoid cells and erythroid cells (Kyba et al., 2002; Pilat et al., 2005), and can lead to a significant risk of leukemogenesis in large animals (Zhang et al., 2008). Although a tetracycline-inducible HoxB4 expression system has been utilized to overcome these unwanted effects, this gene expression system is complex, and cannot be directly applied to therapeutic use. Foreign genes can be integrated into the host chromosome in a stable gene expression system that includes a tetracycline-regulated system, and this could cause an increased risk of cellular transformation (Li et al., 2002; Hacein-Bey-Abina et al., 2003; Williams and Baum, 2004). Therefore, to apply ES cell- and iPS cell-derived HSPCs to clinical medicine, development of a simple and transient HoxB4 transduction method in ES and iPS cells is required.

We have utilized an adenovirus (Ad) vector as a tool for transduction of functional genes into stem cells, because Ad vectors are relatively easy to construct, can be produced at high titers, and mediate efficient and transient gene expression in both dividing and nondividing cells. We have demonstrated that Ad vectors could efficiently transduce a foreign gene in stem cells, including ES and iPS cells (Kawabata et al., 2005; Tashiro et al., 2009, 2010). We also succeeded in promoting the differentiation of osteoblasts, adipocytes, or hepatoblasts from ES and iPS cells by Ad vector-mediated transient transduction of Runx2, PPARγ, or Hex, respectively (Tashiro et al., 2009, 2008; Inamura et al., 2011).

Our data led us to examine whether HSPCs could also be efficiently differentiated from ES and iPS cells by Ad vector-mediated transduction of a HoxB4. In the present study, we investigated whether or not differentiation of HSPCs from mouse ES and iPS cells could be promoted by transient HoxB4 expression. Our results showed that Ad vector-mediated transient HoxB4 expression in mouse ES and iPS cells are sufficient to augment the differentiation of hematopoietic cells, including HSPCs, from mouse ES and iPS cells. This result indicates that an Ad vector-mediated transient gene expression system would be a powerful and safe tool to induce hematopoietic differentiation from mouse ES and iPS cells.

Results

Transduction with Ad vectors in ES-EBs or iPS-EBs

A previous study using a tetracycline-inducible HoxB4 expression system showed that hematopoietic stem/progenitor cells (HSPCs) were generated by induction of HoxB4 expression in ES cell-derived embryoid bodies (ES-EBs) from day 4 to day 6 of differentiation (Kyba et al., 2002), suggesting that HoxB4 expression within this time range would be effective for induction of hematopoietic cells. In addition, $CD41^+c\text{-}kit^+$ cells in EBs are reported to be early hematopoietic progenitor cells (Mitjavila-Garcia et al., 2002; Mikkola et al., 2003). Thus, we planned to transduce HoxB4 in total cells derived from ES- or iPS-EBs on day 5 of differentiation or in $CD41^+c\text{-}kit^+$ cells derived from ES- or iPS-EBs on day 6. We initially investigated the expression of coxsackievirus and adenovirus receptor (CAR) in ES-EB- or iPS-EB-derived cells, because CAR was indispensable for transduction of an exogenous gene using Ad vector (Bergelson et al., 1997; Tomko et al., 1997). Flow cytometric analysis showed the expression of CAR in ES-EB- and iPS-EB-derived total cells and $CD41^+c\text{-}kit^+$ cells, although the expression levels of CAR in $CD41^+c\text{-}kit^+$ cells were decreased in comparison with that in total cells (Figs. 1a and b). These results indicate that ES-EB- and iPS-EB-derived total cells and $CD41^+c\text{-}kit^+$ cells could be transduced with Ad vectors. We also observed the expression of green fluorescent protein (GFP) in iPS-EB-derived total cells. Because the mouse iPS cells used in this study express GFP under the control of Nanog promoter (Okita et al., 2007), the existence of GFP-positive cells showed that undifferentiated iPS cells would still be present in iPS-EB-derived total cells.

We next examined the transduction efficiency in EB-derived total cells or EB-derived $CD41^+c\text{-}kit^+$ cells using DsRed- or GFP-expressing Ad vectors, respectively. After transduction with Ad-DsRed or Ad-GFP at 3000 vector particles (VPs)/cell, the cells were cultured with the hematopoietic cytokines for 2 days. The results showed that, at 3000 VPs/cell, approximately 60% or 40% of the EB-derived total cells or EB-derived $CD41^+c\text{-}kit^+$ cells, respectively, expressed transgenes (Figs. 1c and d). Although the number of transgene-expressing cells was increased in the case of transduction with Ad vectors at 10,000 VPs/cell, the number of viable cells was markedly reduced (data not shown). Therefore, we decided to use Ad vectors at 3000 VPs/cell for transducing human HoxB4 (hHoxB4) into ES-EBs and iPS-EBs. RT-PCR analysis on day 3 after transduction with Ad-hHoxB4 into EB-derived total cells showed an elevation of hHoxB4 mRNA expression in hHoxB4-transduced cells, while neither non-transduced cells nor LacZ-transduced cells showed hHoxB4 expression (Fig. 1e). Importantly, the expression level of hHoxB4 in the cells was markedly decreased on day 6 after Ad

transduction. This result showed that the ES-EB- or iPS-EB-derived cells could express transgenes by Ad vectors, and that Ad vector mediated the transient transgene expression in these cells.

Transient HoxB4 expression augments the generation of hematopoietic cells from mouse ES and iPS cells

To induce and expand the hematopoietic cells from the iPS cell line 38C2, EB-derived total cells were plated and cultured on OP9 stromal cells with the hematopoietic cytokines. On day 10 after plating on OP9 cells, the number of 38C2-derived hematopoietic cells in LacZ-transduced cells was similar to that in non-transduced cells. On the other hand, transient transduction of HoxB4 with Ad-hHoxB4 resulted in a significant increase in the number of hematopoietic cells compared with non-transduced cells or LacZ-transduced cells (Fig. 2a, middle). Likewise, an increase in the hematopoietic cell number by Ad vector-mediated hHoxB4 transduction was also observed in ES cell derived-hematopoietic cells or the other iPS line 20D17-derived hematopoietic cells (Fig. 2a, left and right). Additionally, ES-EB- or iPS-EB-derived CD41$^+$c-kit$^+$ cells, which were transiently transduced with hHoxB4, could proliferate on OP9 stromal cells for over 20 days (Fig. 2b). This result is mostly in agreement with the previous report that ES cell-derived hematopoietic cells stably expressing HoxB4 had a growth advantage in the presence of hematopoietic cytokines (Pilat et al., 2005). Transient, but not stable, HoxB4 expression in ES-EB- or iPS-EB-derived cells would be sufficient to augment the generation of hematopoietic cells from ES and iPS cells.

We next investigated the surface antigen expression in non-transduced cells, LacZ-transduced cells, or hHoxB4-transduced cells after expansion on OP9 stromal cells. Flow cytometric analysis revealed an increase of CD45 and CD41 expressions in HoxB4-transduced cells, compared with non-transduced cells and LacZ-transduced cells (Figs. 3a and b). CD45 is known as a marker of hematopoietic cells. In both *in vitro* ES cell differentiation and a developing mouse embryo, the expression of CD45 was developmentally controlled, and CD45 expression was observed on hematopoietic cells after expression of CD41 (Mitjavila-Garcia et al., 2002; Mikkola et al., 2003). Thus, a higher percentage of CD45$^+$ cells in HoxB4-transduced cells would be due, at least in part, to an increase of CD41 expression in HoxB4-transduced cells relative to non-transduced cells and LacZ-transduced cells. We also found a significant elevation of Sca-1 in hHoxB4-transduced cells (Figs. 3a and b). Sca-1 is expressed in fetal and adult HSPCs (Arai et al., 2004; McKinney-Freeman et al., 2009), although Sca-1 expression was observed in other types of cells. Therefore, our data suggest that immature hematopoietic cells would be generated in hHoxB4-transduced cells more efficiently than in non-transduced cells or LacZ-transduced cells.

In parallel with the flow cytometric analysis, we also analyzed the expression levels of hematopoietic marker genes in iPS cell-derived hematopoietic cells by RT-PCR (Fig. 3c). The expression levels of marker genes in LacZ-transduced cells were mostly equal to those in non-transduced cells. In contrast, among the genes we assayed, the expression levels of *Gata-1*, *c-myb*, and *Cxcr4* mRNA were slightly but significantly up-regulated in hHoxB4-transduced cells. GATA-1 reflects early hematopoietic development, whereas c-Myb is a marker of definitive hematopoiesis (Godin and Cumano, 2002). Increased expression of these genes in HoxB4-transduced cells suggests that transient hHoxB4 expression promotes the production of both primitive and definitive hematopoietic progenitor cells from mouse ES and iPS cells. We could not detect the hHoxB4 mRNA expression in Ad-hHoxB4-transduced cells, confirming the transient hHoxB4 expression by Ad vectors (Fig. 3c).

HoxB4 expression enhances development of hematopoietic progenitor cells from mouse ES and iPS cells

To examine whether hematopoietic immature cells with hematopoietic colony-forming potential could be generated from ES and iPS cells, ES cell-derived hematopoietic cells and iPS cell-derived hematopoietic cells, both of which were cultured on OP9 stromal cells for 10 days, were plated and cultured in methylcellulose-containing media with hematopoietic cytokines. Without Ad transduction, the number of total hematopoietic colonies in the iPS cell line 38C2 was five times as high as that in ES cells, whereas another iPS cell line, 20D17, had nearly the same hematopoietic differentiation potential as ES cells (Fig. 4a). These results indicate that there is a difference in hematopoietic differentiation potential among iPS cell lines.

We next examined the hematopoietic colony potential in LacZ-transduced cells or HoxB4-transduced cells. The colony assay revealed a significant increase in the number of total hematopoietic colonies in hHoxB4-transduced cells compared with control cells, whereas there was no significant difference in the number of hematopoietic colonies between non-transduced cells and LacZ-transduced cells (Fig. 4a). Note that the number of the most immature multipotent progenitor cells, CFU-GEMM/CFU-Mix, in hHoxB4-transduced cells was approximately seven times as great as that in non-transduced cells or LacZ-transduced cells, and that large CFU-Mix colonies were more frequently observed in hHoxB4-transduced cells than control cells (Fig. 4b and data not shown). A colony assay after culturing on OP9 stromal cells for 20 days also revealed that much number of myeloid (CFU-G, M, and GM) colonies and CFU-Mix colonies were observed by transient hHoxB4 transduction (Figs. 4c and d). Thus, our data clearly showed that Ad vector-mediated transient hHoxB4 expression

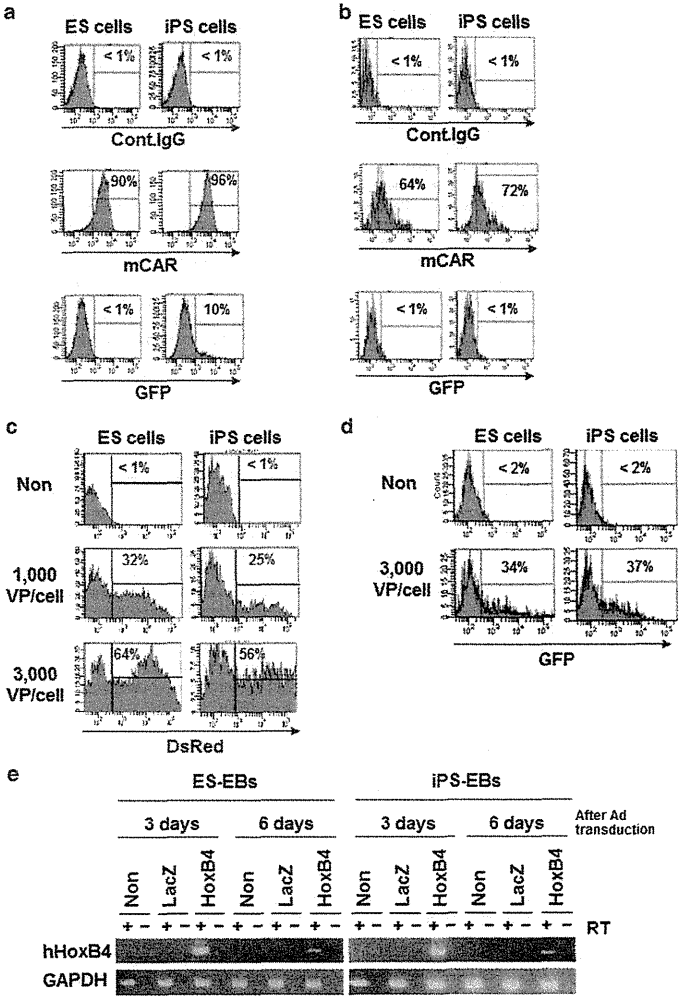

Figure 1 Transduction with Ad vectors in ES-EB- or iPS-EB-derived cells. (a, b) The expression levels of CAR, a primary receptor for Ad, in ES-EB- or iPS-EB-derived total cells (a) or CD41$^+$c-kit$^+$ cells (b) were detected with anti-mouse CAR monoclonal antibody by flow cytometric analysis. As a negative control, the cells were incubated with an irrelevant antibody. Data shown are from one representative experiment of three performed. (c, d) EB-derived total cells (c) or CD41$^+$c-kit$^+$ cells (d), purified by FACS (Supplemental Fig. 1), were transduced with Ad-DsRed or Ad-GFP for 1.5 h, and transgene-expressing cells were then analyzed by flow cytometry. Because CD41$^+$c-kit$^+$ cells do not express GFP (Fig. 1b), Ad-GFP was used for transduction into CD41$^+$c-kit$^+$ cells. Similar results were obtained in three independent experiments. (e) The expression level of human HoxB4 mRNA in the cells was examined by conventional RT-PCR on days 3 and 6 after transduction with Ad-hHoxB4 at 3000 VPs/cell into EB-derived total cells. Abbreviations: ES, embryonic stem; iPS, induced pluripotent stem; mCAR, mouse coxsackievirus and adenovirus receptor; GFP, green fluorescent protein; Cont., control.; VP, vector particle; RT, reverse transcription; GAPDH, glyceraldehyde-3-phosphate dehydrogenase.Transduction with Ad vectors

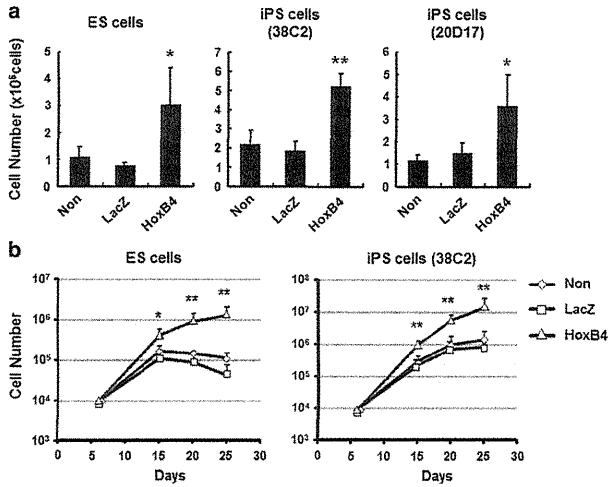

Figure 2 The number of ES cell- or iPS cell-derived hematopoietic cells was significantly increased in Ad-hHoxB4-transduced cells. (a, b) ES-EB- or iPS-EB-derived total cells (a) or CD41$^+$c-kit$^+$ cells (b) were transduced with Ad-LacZ or Ad-hHoxB4 at 3000 VPs/cell for 1.5 h, and the cells were then plated on OP9 feeder cells. As a control, non-transduced cells were also plated on OP9 cells. After culturing on OP9 feeders with the hematopoietic cytokines for 10 days (a) or 20 days (b), the number of hematopoietic cells per 2 wells of a 6-well plate was counted. (a) Left, ES cells; middle, iPS cell line 38C2; right, iPS cell line 20D17. Results shown were the mean of four independent experiments with indicated standard deviations. * $p<0.05$, ** $p<0.01$ as compared with non-transduced or Ad-LacZ-transduced cells.

enhances the differentiation of hematopoietic immature cells, including HSPCs, from mouse ES and iPS cells.

Discussion

Previous studies have shown that enforced expression of HoxB4 is an effective strategy for hematopoietic differentiation from both mouse and human ES cells (Kyba et al., 2002; Bowles et al., 2006; Pilat et al., 2005; Schiedlmeier et al., 2007). These studies usually used recombinant ES cells, such as ES cells constitutively expressing HoxB4 (Pilat et al., 2005) or ES cells containing a tetracycline (Tet)-inducible HoxB4 expression system (Kyba et al., 2002), to induce hematopoietic cells. However, this expression system might raise clinical concerns, including the risk of oncogenesis due to integration of transgenes into host genomes. In the present study, we showed that Ad vector-mediated transient hHoxB4 expression in mouse ES-EB- or iPS-EB-derived cells could result in an efficient production of hematopoietic cells, including HSPCs with a hematopoietic colony-forming ability, from mouse ES and iPS cells (Figs. 2, 3, and 4). Our data obtained in this report are largely consistent with previous reports (Kyba et al., 2002) in which HSPCs were generated by using ES cells containing the Tet-regulated HoxB4 expression cassette. Therefore, a transient HoxB4 expression system using an Ad vector, instead of a Tet-inducible HoxB4 expression system, would contribute to safer clinical applications of ES or iPS cell-derived hematopoietic cells.

Conventional Ad vector is known to infect the cells through an entry receptor, CAR, on the cellular surface (Bergelson et al., 1997; Tomko et al., 1997). Previously, we showed that undifferentiated ES and iPS cells expressed CAR, and conventional Ad vector could easily transduce a foreign gene in more than 90% of the undifferentiated ES and iPS cells at 3000 VPs/cell (Kawabata et al., 2005; Tashiro et al., 2009). Like undifferentiated ES and iPS cells, we could detect the CAR expression in more than 90% or 70% of EB-derived total cells or EB-derived CD41$^+$c-kit$^+$ cells, respectively (Figs. 1a and b). However, the transduction efficiency in EB-derived total cells or CD41$^+$c-kit$^+$ cells was only 60% or 40%, respectively, of the cells at most (Figs. 1c and d). Although we are not certain why transgene expression was not observed in all of CAR$^+$ EB-derived cells, it is possible that the promoter might not have worked in all of the cells because the EB-derived total cells and CD41$^+$c-kit$^+$ cells were heterogeneous, unlike in the case of undifferentiated ES and iPS cells. It is also possible that the Ad binding site of CAR might be disrupted by trypsin treatment during the preparation of the EB-derived cells (Carson, 2000). Because the development of efficient transduction methods in EB-derived cells is considered to be a powerful tool to promote the hematopoietic differentiation from ES and iPS cells, further improvement of the transduction conditions will be needed.

We found a difference in the hematopoietic differentiation potential among mouse iPS cell lines (Fig. 4). Consistent with our data, Kulkeaw et al. showed a difference in the hematopoietic differentiation capacity among six iPS cell lines (Kulkeaw et al., 2010). In addition, recent studies have reported that iPS cells leave an epigenetic memory of

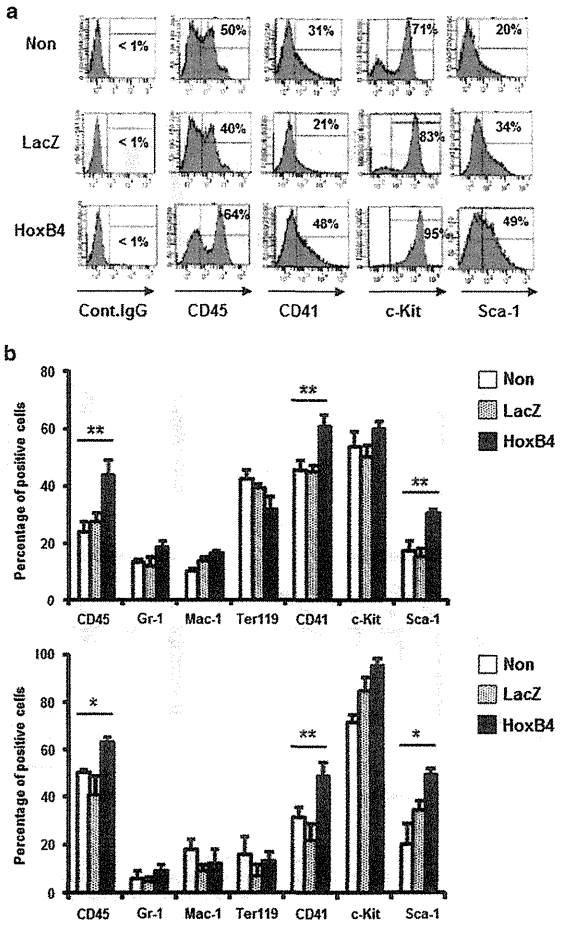

Figure 3 Expression of surface antigen and hematopoietic marker genes in mouse ES cell- or iPS cell-derived cells. (a, b) ES cell- or iPS cell line 38C2-derived cells were reacted with each antibody, and were then subjected to flow cytometric analysis. (a) Representative data from iPS cell line 38C2 are shown. (b) Percentage of each antigen positive cells in ES cell-derived cells (upper) or iPS cell-derived cells (lower) is shown. The data expressed the mean of three independent experiments with indicated standard deviations. * $p<0.05$, ** $p<0.01$ as compared with non-transduced or Ad-LacZ-transduced cells. (c) Total RNA was extracted from undifferentiated iPS cells (Day 0), iPS-EB (Day 5), iPS cells-derived hematopoietic cells (day 15), OP9 stromal cells, and MEF feeder, and semi-quantitative PCR (left) or quantitative real-time PCR (right) was then carried out as described in the Materials and methods. The data expressed the mean of three independent experiments with indicated standard deviations. * $p<0.05$, ** $p<0.01$ as compared with non-transduced or Ad-LacZ-transduced cells. Abbreviation: EBs, embryoid bodies; MEF, mouse embryonic fibroblast; GATA, GATA-binding protein.

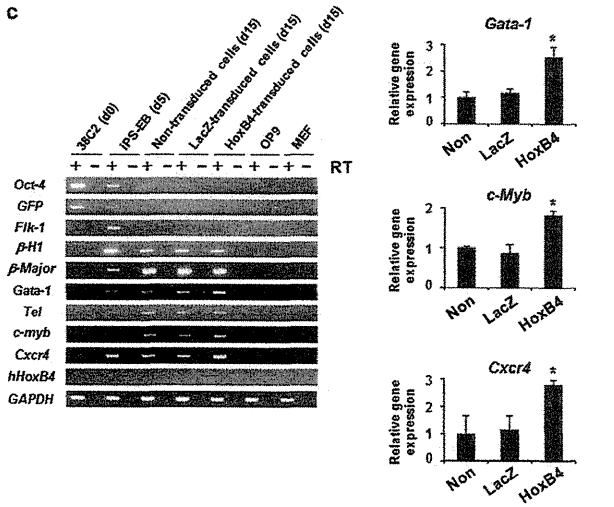

Figure 3 (*continued*).

their cellular origin, and this memory influences their functional properties, including *in vitro* differentiation (Kim et al., 2010; Polo et al., 2010). Thus, these reports indicate that, in order to obtain a large number of HSPCs from iPS cells, it is necessary to choose an appropriate iPS cell line, such as HSPC-derived iPS cells (Okabe et al., 2009). Importantly, using mouse embryonic fibroblast-derived iPS cells (38C2 and 20D17), we showed that the use of transient hHoxB4 transduction in iPS-EB-derived cells achieved more effective differentiation into HSPCs than the use of non-transduced cells (Fig. 4). Our method therefore should be efficient for the production of HSPCs from any iPS cell line.

An important but unsolved question in this study is whether ES cell-derived hematopoietic cells and iPS cell-derived hematopoietic cells transduced with Ad-hHoxB4 have long-term hematopoietic reconstitution potential *in vivo*. Recent studies have demonstrated that some surface antigen expressions were different between bone marrow-derived HSPCs and ES cell-derived HSPCs, and that CD41$^+$ cells had long-term repopulation ability in ES cell-derived HSPCs (McKinney-Freeman et al., 2009; Matsumoto et al., 2009). Our flow cytometric analysis revealed an increase of CD41$^+$ cells in hHoxB4-transduced cells compared with non-transduced cells and LacZ-transduced cells (Fig. 3b). We also showed that Ad-hHoxB4-transduced cells could proliferate on OP9 stromal cells more efficiently than control cells (Fig. 2). Thus, these results suggest that immature hematopoietic cells were generated by transient hHoxB4 transduction, and that hHoxB4-transduced cells might have reconstitution potential *in vivo*. This *in vivo* transplantation analysis is now on-going in our laboratory.

In the present study, we succeeded in the promotion of hematopoietic differentiation from mouse ES and iPS cells by Ad vector-mediated hHoxB4 transduction. Ad vector transduction can avoid the integration of transgene into host genomes, and multiple genes can be transduced by Ad vectors in an appropriate differentiation period. Thus, an even more efficient protocol for hematopoietic differentiation from ES and iPS cells could likely be established by co-transduction of HoxB4 and other genes involved in the hematopoiesis, such as Cdx4 (Wang et al., 2005) and Scl/Tal1 (Kurita et al., 2006), using Ad vectors. Taken together, our results show that Ad vector-mediated transient gene expression is valuable tool to induce hematopoietic cell from ES and iPS cells, and this strategy would be applicable to safe therapeutic applications, such as HSPC transplantation.

Materials and methods

Antibodies

The following primary monoclonal antibodies (Abs), conjugated with fluorescein isothiocyanate (FITC), phycoerythrin (PE), allophycocyanin (APC), or PE-Cy7, were used for flow cytometric analysis: anti-CD45 (30-F11, eBioscience, San Diego, CA), anti-CD11b (M1/70, eBioscience), anti-Sca-1 (D7, eBioscience), anti-Ter-119 (Ter-119, eBioscience), anti-Gr-1 (RB6-8C5, eBioscience), anti-c-Kit (ACK2 or 2B8, eBioscience), anti-CD41 (MWReg30, BD Bioscience San Jose, CA). Purified rat anti-coxsackievirus and adenovirus receptor (CAR) was kindly provided from Dr. T. Imai (KAN Research Institute, Hyogo, Japan). For detection of CAR, the PE-conjugated donkey anti-rat IgG (Jackson ImmunoResearch Laboratories, West Grove, PA) or DyLight649-conjugated goat anti-rat IgG (BioLegend, San Diego, CA) was used as secondary Abs.

Cell cultures

The mouse ES cell line E14 and two mouse iPS cell lines, 38C2 and 20D17, both of which were generated by Yamanaka and his colleagues (Okita et al., 2007), were used in this study. 38C2 was kindly provided by Dr. S. Yamanaka (Kyoto University, Kyoto, Japan), and 20D17 was purchased from Riken Bioresource Center (Tsukuba, Japan). In the present study, we mainly used 38C2 iPS cells except where otherwise indicated. Mouse ES and iPS cells were cultured in leukemia inhibitory factor-containing medium on a feeder layer of mitomycin C-inactivated mouse embryonic fibroblasts (MEF) as described previously (Tashiro et al., 2009). OP9 stromal cells were cultured in α-minimum essential medium (αMEM: Sigma, St. Louis, MO) supplemented with 20% fetal bovine serum (FBS), 2 mM L-glutamine (Invitrogen, Carlsbad, CA), and non-essential amino acid (Invitrogen).

Ad vectors

Ad vectors were constructed by an improved *in vitro* ligation method (Mizuguchi and Kay, 1998, 1999). The shuttle

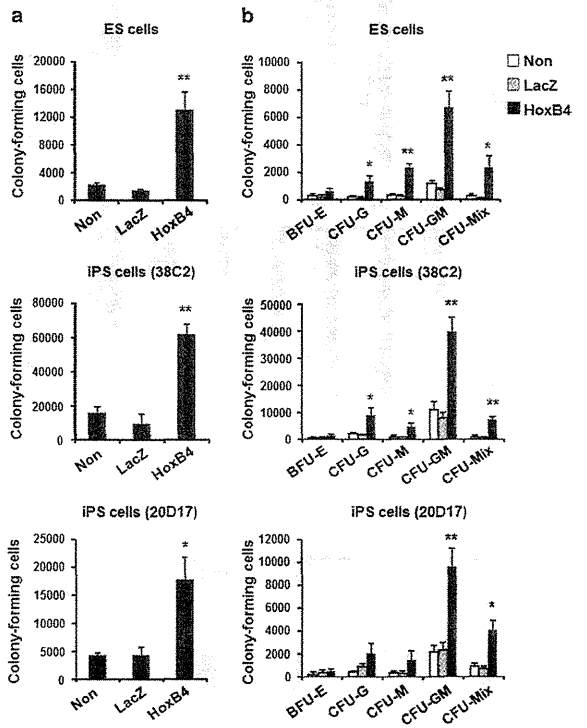

Figure 4 Significant increase of hematopoietic colony-forming cells in Ad-HoxB4-transduced hematopoietic cells. After ES-EB- or iPS-EB-derived cells were transduced with Ad-LacZ or Ad-hHoxB4, hematopoietic cells were generated by co-culturing with OP9 cells in the presence of hematopoietic cytokines for 10 days (a, b) or 20 days (c, d). A colony-forming assay was performed using methylcellulose medium, and the number of hematopoietic colonies was then counted under light microscopy. The number of total colonies (a, c) or subdivided colonies by morphological subtype (BFU-E, CFU-G, CFU-M, CFU-GM, and CFU-Mix) (b, d) generated from ES cells (E14) or iPS cells (38C2 and 20D17) was shown. Colony number was normalized to total number of the cells. Results shown were the mean of three (c, d) or four (a, b) independent experiments with indicated standard deviations. * $p<0.05$, ** $p<0.01$ as compared with non-transduced or Ad-LacZ-transduced cells. Abbreviation: BFU-E, burst-forming unit; CFU-G, colony-forming unit-granulocyte; CFU-M, CFU-monocyte; CFU-GM, CFU-granulocyte, monocyte; CFU-GEMM/CFU-Mix, CFU-granulocyte, erythrocyte, monocyte, megakryocyte.

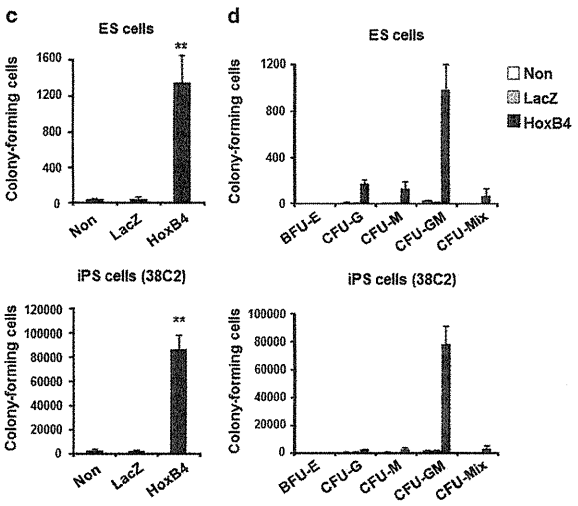

Figure 4 (*continued*).

plasmid pHMCA5, which contains the CMV enhancer/β-actin promoter with β-actin intron (CA) promoter (a kind gift from Dr. J. Miyazaki, Osaka University, Osaka, Japan) (Niwa et al., 1991), was previously constructed (Kawabata et al., 2005). The human HoxB4 (hHoxB4)-expressing plasmid, pHMCA-hHoxB4, and DsRed-expressing plasmid, pHMCA-DsRed, were generated by inserting a hHoxB4 cDNA (a kindly gift from Dr. S. Karlsson, Lund University Hospital, Lund, Sweden) and a DsRed cDNA (Clontech, Mountain View, CA), respectively, into pHMCA5. pHMCA-hHoxB4 or pHMCA-DsRed were digested with I-*Ceu*I/PI-*Sce*I and ligated into I-*Ceu*I/PI-*Sce*I-digested pAdHM4 (Mizuguchi and Kay, 1998), resulting in pAd-hHoxB4 or pAd-DsRed, respectively. Ad-hHoxB4 and Ad-DsRed were generated and purified as described previously (Tashiro et al., 2008). The CA promoter-driven β-galactosidase (LacZ)-expressing Ad vector, Ad-LacZ, and the CA promoter-driven GFP-expressing Ad vector, Ad-CA-GFP, were generated previously (Tashiro et al., 2008). The vector particle (VP) titer was determined by using a spectrophotometrical method (Maizel et al., 1968).

In vitro differentiation

Prior to embryoid body (EB) formation, mouse ES or iPS cells were suspended in differentiation medium (Dulbecco's modified Eagle's medium (Wako, Osaka, Japan) containing 15% FBS, 0.1 mM 2-mercaptoethanol (Nacalai tesque, Kyoto, Japan), 1×non-essential amino acid (Specialty Media, Inc.), 1×nucleosides (Specialty Media, Inc.), 2 mM L-glutamine (Invitrogen), and penicillin/streptomycin (Invitrogen)) and cultured on a culture dish at 37 °C for 45 min to remove MEF layers. Mouse ES cell- or iPS cell-derived EBs (ES-EBs or iPS-EBs, respectively) were generated by culturing ES or iPS cells on a round-bottom low cell binding 96-well plate (Lipidure-coat plate; Nunc) at 1×10^3 cells per well. ES-EBs or iPS-EBs were collected on day 5, and a single cell suspension was prepared by trypsin/EDTA treatment (Invitrogen) at 37 °C for 2 min. ES-EB- or iPS-EB-derived CD41$^+$c-kit$^+$ cells were sorted by FACSAria (BD Bioscience). The purity of the CD41$^+$c-kit$^+$ cells was greater than 90% based on flow cytometric analysis (Supplemental Fig. 1). Cells were then transduced with an Ad vector at 3000 vector particles (VPs)/cell for 1.5 h in a 15 ml tube. After transduction, total cells (2×10^5) or CD41$^+$c-kit$^+$ cells (1×10^4) were cultured on OP9 feeder cells in a well of a 6-well plate in αMEM supplemented with 20% FBS, 2 mM L-glutamine, non-essential amino acid, 0.05 mM 2-mercaptoethanol, and hematopoietic cytokines (50 ng/ml mouse stem cell factor (SCF), 50 ng/ml human Flt-3 ligand (Flt-3L), 20 ng/ml thrombopoietin (TPO), 5 ng/ml mouse interleukin (IL)-3, and 5 ng/ml human IL-6 (all from Peprotec, Rocky Hill, NJ)). After culturing with OP9 stromal cells, both non-adherent hematopoietic cells and adherent hematopoietic cells were collected as follows. The non-adherent hematopoietic cells were collected by pipetting and were transferred to 15 ml tubes. The adherent hematopoietic cells were harvested with the use of trypsin/EDTA, and then incubated in a tissue culture dish for 30 min to eliminate the OP9 cells. Floating cells were collected as hematopoietic cells and transferred to the same 15 ml tubes. These hematopoietic cells were kept on ice for further analysis.

Flow cytometry

Cells (1×10^5 to 5×10^5) were incubated with monoclonal Abs at 4 °C for 30 min and washed twice with staining buffer (PBS/2%FBS). Dead cells were excluded from the analysis by 7-amino actinomycin D (7-AAD, eBioscience). Analysis was performed on an LSRFortessa flow cytometer by using FACS-Diva software (BD Bioscience). For detection of transgene expression by Ad vectors, EB-derived total cells or CD41$^+$c-kit$^+$ cells were transduced with Ad-DsRed or Ad-CA-GFP, respectively, for 1.5 h. At 48 h of incubation with the hematopoietic cytokines as described above, transgene expression in the cells was analyzed by flow cytometry.

Table 1 List of primers used for RT-PCR.

Gene name	Species	(5′) Sense primers (3′)	(5′)Antisense primers (3′)
GAPDH	Ms	ACCACAGTCCATGCCATCAC	TCCACCACCCTGTTGCTGTA
HoxB4	Hs	AGAGGCGAGAGAGCAGCTT	TTCCTTCTCCAGCTCCAAGA
Oct-3/4	Ms	GTTTGCCAAGCTGCTGAAGC	TCTAGCCCAAGCTGATTGGC
GFP	–	CACATGAAGCAGCACGACTT	TGCTCAGGTAGTGGTTGTCG
Flk-1	Ms	TCTGTGGTTCTGCGTGGAGA	GTATCATTTCCAACCACCC
Gata1	Ms	TTGTGAGGCCAGAGAGTGTG	TTCCTCGTCTGGATTCCATC
Gata1 (real-time PCR)	Ms	GTCAGAACCGGCCTCTCATC	GTGGTCGTTTGACAGTTAGTGCAT
Tel	Ms	CTGAAGCAGAGGAAATCTCGAATG	GGCAGGCAGTGATTATTCTCGA
c-myb	Ms	CCTCACCTCCATCTCAGCTC	GCTGGTGAGGCACTTTCTTC
β-H1	Ms	AGTCCCCATGGAGTCAAAGA	CTCAAGGAGACCTTTGCTCA
β-Major	Ms	CTGACAGATGCTCTCTTGGG	CACAACCCCAGAAACAGACA
CXCR4	Ms	GTCTATGTGGGCGTCTGGAT	GGCAGAGCTTTTGAACTTGG

Colony assay

A colony-forming assay was performed by plating ES cell-derived hematopoietic cells or iPS cell-derived hematopoietic cells into methylcellulose medium M3434 (Stem Cell Technologies, Vancouver, BC, Canada). After incubation at 37 °C and 5% CO_2 for 10 to 14 days in a humidified atmosphere, colony numbers were counted. The morphology of colonies was observed using an inverted light microscope.

RT-PCR

Total RNA was isolated with the use of ISOGENE (Nippon Gene, Tokyo, Japan). cDNA was synthesized by using Super-Script II reverse transcriptase (Invitrogen) and the oligo(dT) primer. Semi-quantitative PCR was performed with the use of TaKaRa ExTaq HS DNA polymerase (Takara, Shiga, Japan). The PCR conditions were 94 °C for 2 min, followed by the appropriate number of cycles of 94 °C for 15 s, 55 °C for 30 s with 72 °C for 30 s and a final extension of 72 °C for 1 min, except for the addition of 5% dimethyl sulfoxide in the case of hHoxB4 cDNA amplification. The product was assessed by 2% agarose gel electrophoresis followed by ethidium bromide staining. Quantitative real-time PCR was performed using StepOnePlus real-time PCR system with FAST SYBR Green Master Mix (Applied Biosystems, Foster-City, CA). The sequences of the primers used for in this study are listed in Table 1.

Supplementary materials related to this article can be found online at doi:10.1016/j.scr.2011.09.001.

Conflict of interest

The authors have no financial conflict of interest.

Acknowledgments

We thank Dr. S. Yamanaka for kindly providing the mouse iPS cell line 38C2 and 20D17. We would also like to thank Dr. J. Miyazaki and Dr. T. Imai for providing the CA promoter and anti-mouse CAR monoclonal antibody, respectively. We also thank Dr. K. Nishikawa (National Institute of Biomedical Innovation) for helpful comments. This work was supported by grants from the Ministry of Education, Culture, Sports, Science, and Technology (MEXT) of Japan and the Ministry of Health, Labour, and Welfare of Japan.

References

Arai, F., Hirao, A., Ohmura, M., Sato, H., Matsuoka, S., Takubo, K., Ito, K., Koh, G.Y., Suda, T., 2004. Tie2/angiopoietin-1 signaling regulates hematopoietic stem cell quiescence in the bone marrow niche. Cell 118, 149 161.

Bergelson, J.M., Cunningham, J.A., Droguett, G., Kurt-Jones, E.A., Krithivas, A., Hong, J.S., Horwitz, M.S., Crowell, R.L., Finberg, R.W., 1997. Isolation of a common receptor for Coxsackie B viruses and adenoviruses 2 and 5. Science 275, 1320 1323.

Bowles, K.M., Vallier, L., Smith, J.R., Alexander, M.R., Pedersen, R.A., 2006. HOXB4 overexpression promotes hematopoietic development by human embryonic stem cells. Stem Cells 24, 1359–1369.

Carson, S.D., 2000. Limited proteolysis of the coxsackievirus and adenovirus receptor (CAR) on HeLa cells exposed to trypsin. FEBS Lett. 484, 149–152.

Chadwick, K., Wang, L., Li, L., Menendez, P., Murdoch, B., Rouleau, A., Bhatia, M., 2003. Cytokines and BMP-4 promote hematopoietic differentiation of human embryonic stem cells. Blood 102, 906 915.

Evans, M.J., Kaufman, M.H., 1981. Establishment in culture of pluripotential cells from mouse embryos. Nature 292, 154 156.

Godin, I., Cumano, A., 2002. The hare and the tortoise: an embryonic haematopoietic race. Nat. Rev. Immunol. 2, 593–604.

Haceìn-Bey-Abina, S., Von Kalle, C., Schmidt, M., McCormack, M.P., Wulffraat, N., Leboulch, P., Lim, A., Osborne, C.S., Pawliuk, R., Morillon, E., Sorensen, R., Forster, A., Fraser, P., Cohen, J.I., de Saint Basile, G., Alexander, I., Wintergerst, U., Frebourg, T., Aurias, A., Stoppa-Lyonnet, D., Romana, S., Radford-Weiss, I., Gross, F., Valensi, F., Delabesse, E., Macintyre, E., Sigaux, F., Soulier, J., Leiva, L.E., Wissler, M., Prinz, C., Rabbitts, T.H., Le Deist, F., Fischer, A., Cavazzana-Calvo, M., 2003. LMO2-associated clonal T cell proliferation in two patients after gene therapy for SCID-X1. Science 302, 415–419.

Inamura, M., Kawabata, K., Takayama, K., Tashiro, K., Sakurai, F., Katayama, K., Toyoda, M., Akutsu, H., Miyagawa, Y., Okita, H., Kiyokawa, N., Umezawa, A., Hayakawa, T., Furue, M.K., Mizuguchi, H., 2011. Efficient generation of hepatoblasts from human ES cells and iPS cells by transient overexpression of homeobox gene HEX. Mol. Ther. 19, 400 407.

Kawabata, K., Sakurai, F., Yamaguchi, T., Hayakawa, T., Mizuguchi, H., 2005. Efficient gene transfer into mouse embryonic stem cells with adenovirus vectors. Mol. Ther. 12, 547 554.

Keller, G., 2005. Embryonic stem cell differentiation: emergence of a new era in biology and medicine. Genes Dev. 19, 1129–1155.

Kim, K., Doi, A., Wen, B., Ng, K., Zhao, R., Cahan, P., Kim, J., Aryee, M.J., Ji, H., Ehrlich, L.I., Yabuuchi, A., Takeuchi, A., Cunniff, K.C., Hongguang, H., McKinney-Freeman, S., Naveiras, O., Yoon, T.J., Irizarry, R.A., Jung, N., Seita, J., Hanna, J., Murakami, P., Jaenisch, R., Weissleder, R., Orkin, S.H., Weissman, I.L., Feinberg, A.P., Daley, G.Q., 2010. Epigenetic memory in induced pluripotent stem cells. Nature 467, 285 290.

Kulkeaw, K., Horio, Y., Mizuochi, C., Ogawa, M., Sugiyama, D., 2010. Variation in hematopoietic potential of induced pluripotent stem cell lines. Stem Cell Rev. 6, 381–389.

Kurita, R., Sasaki, E., Yokoo, T., Hiroyama, T., Takasugi, K., Imoto, H., Izawa, K., Dong, Y., Hashiguchi, T., Soda, Y., Maeda, T., Suehiro, Y., Tanioka, Y., Nakazaki, Y., Tani, K., 2006. Tal1/Scl gene transduction using a lentiviral vector stimulates highly efficient hematopoietic cell differentiation from common marmoset (*Callithrix jacchus*) embryonic stem cells. Stem Cells 24, 2014 2022.

Kyba, M., Perlingeiro, R.C., Daley, G.Q., 2002. HoxB4 confers definitive lymphoid-myeloid engraftment potential on embryonic stem cell and yolk sac hematopoietic progenitors. Cell 109, 29 37.

Li, Z., Dullmann, J., Schiedlmeier, B., Schmidt, M., von Kalle, C., Meyer, J., Forster, M., Stocking, C., Wahlers, A., Frank, O., Ostertag, W., Kuhlcke, K., Eckert, H.G., Fehse, B., Baum, C., 2002. Murine leukemia induced by retroviral gene marking. Science 296, 497.

Maizel Jr., J.V., White, D.O., Scharff, M.D., 1968. The polypeptides of adenovirus. I. Evidence for multiple protein components in the virion and a comparison of types 2, 7A, and 12. Virology 36, 115 125.

Matsumoto, K., Isagawa, T., Nishimura, T., Ogaeri, T., Eto, K., Miyazaki, S., Miyazaki, J., Aburatani, H., Nakauchi, H., Ema, H., 2009. Stepwise development of hematopoietic stem cells from embryonic stem cells. PLoS One 4, e4820.

McKinney-Freeman, S.L., Naveiras, O., Yates, F., Loewer, S., Philitas, M., Curran, M., Park, P.J., Daley, G.Q., 2009. Surface antigen phenotypes of hematopoietic stem cells from embryos and murine embryonic stem cells. Blood 114, 268 278.

Mikkola, H.K., Fujiwara, Y., Schlaeger, T.M., Traver, D., Orkin, S.H., 2003. Expression of CD41 marks the initiation of definitive hematopoiesis in the mouse embryo. Blood 101, 508 516.

Mitjavila-Garcia, M.T., Cailleret, M., Godin, I., Nogueira, M.M., Cohen-Solal, K., Schiavon, V., Lecluse, Y., Le Pesteur, F., Lagrue, A.H., Vainchenker, W., 2002. Expression of CD41 on hematopoietic progenitors derived from embryonic hematopoietic cells. Development 129, 2003 2013.

Mizuguchi, H., Kay, M.A., 1998. Efficient construction of a recombinant adenovirus vector by an improved in vitro ligation method. Hum. Gene Ther. 9, 2577 2583.

Mizuguchi, H., Kay, M.A., 1999. A simple method for constructing E1- and E1/E4-deleted recombinant adenoviral vectors. Hum. Gene Ther. 10, 2013 2017.

Nakano, T., Kodama, H., Honjo, T., 1994. Generation of lymphohematopoietic cells from embryonic stem cells in culture. Science 265, 1098–1101.

Niwa, H., Yamamura, K., Miyazaki, J., 1991. Efficient selection for high-expression transfectants with a novel eukaryotic vector. Gene 108, 193–199.

Okabe, M., Otsu, M., Ahn, D.H., Kobayashi, T., Morita, Y., Wakiyama, Y., Onodera, M., Eto, K., Ema, H., Nakauchi, H., 2009. Definitive proof for direct reprogramming of hematopoietic cells to pluripotency. Blood 114, 1764–1767.

Okita, K., Ichisaka, T., Yamanaka, S., 2007. Generation of germline-competent induced pluripotent stem cells. Nature 448, 313 317.

Pilat, S., Carotta, S., Schiedlmeier, B., Kamino, K., Mairhofer, A., Will, E., Modlich, U., Steinlein, P., Ostertag, W., Baum, C., Beug, H., Klump, H., 2005. HOXB4 enforces equivalent fates of ES-cell-derived and adult hematopoietic cells. Proc. Natl. Acad. Sci. U. S. A. 102, 12101–12106.

Polo, J.M., Liu, S., Figueroa, M.E., Kulalert, W., Eminli, S., Tan, K.Y., Apostolou, E., Stadtfeld, M., Li, Y., Shioda, T., Natesan, S., Wagers, A.J., Melnick, A., Evans, T., Hochedlinger, K., 2010. Cell type of origin influences the molecular and functional properties of mouse induced pluripotent stem cells. Nat. Biotechnol. 28, 848–855.

Schiedlmeier, B., Santos, A.C., Ribeiro, A., Moncaut, N., Lesinski, D., Auer, H., Kornacker, K., Ostertag, W., Baum, C., Mallo, M., Klump, H., 2007. HOXB4's road map to stem cell expansion. Proc. Natl. Acad. Sci. U. S. A. 104, 16952–16957.

Schmitt, T.M., de Pooter, R.F., Gronski, M.A., Cho, S.K., Ohashi, P.S., Zuniga-Pflucker, J.C., 2004. Induction of T cell development and establishment of T cell competence from embryonic stem cells differentiated in vitro. Nat. Immunol. 5, 410 417.

Takahashi, K., Yamanaka, S., 2006. Induction of pluripotent stem cells from mouse embryonic and adult fibroblast cultures by defined factors. Cell 126, 663 676.

Takahashi, K., Tanabe, K., Ohnuki, M., Narita, M., Ichisaka, T., Tomoda, K., Yamanaka, S., 2007. Induction of pluripotent stem cells from adult human fibroblasts by defined factors. Cell 131, 861–872.

Tashiro, K., Kawabata, K., Sakurai, H., Kurachi, S., Sakurai, F., Yamanishi, K., Mizuguchi, H., 2008. Efficient adenovirus vector-mediated PPAR gamma gene transfer into mouse embryoid bodies promotes adipocyte differentiation. J. Gene Med. 10, 498–507.

Tashiro, K., Inamura, M., Kawabata, K., Sakurai, F., Yamanishi, K., Hayakawa, T., Mizuguchi, H., 2009. Efficient adipocyte and osteoblast differentiation from mouse induced pluripotent stem cells by adenoviral transduction. Stem Cells 27, 1802–1811.

Tashiro, K., Kawabata, K., Inamura, M., Takayama, K., Furukawa, N., Sakurai, F., Katayama, K., Hayakawa, T., Furue, M.K., Mizuguchi, H., 2010. Adenovirus vector-mediated efficient transduction into human embryonic and induced pluripotent stem cells. Cell. Reprogram. 12, 501 507.

Thomson, J.A., Itskovitz-Eldor, J., Shapiro, S.S., Waknitz, M.A., Swiergiel, J.J., Marshall, V.S., Jones, J.M., 1998. Embryonic stem cell lines derived from human blastocysts. Science 282, 1145–1147.

Tomko, R.P., Xu, R., Philipson, L., 1997. HCAR and MCAR: the human and mouse cellular receptors for subgroup C adenoviruses and group B coxsackieviruses. Proc. Natl. Acad. Sci. U. S. A. 94, 3352 3356.

Vodyanik, M.A., Bork, J.A., Thomson, J.A., Slukvin, I.I., 2005. Human embryonic stem cell-derived CD34+ cells: efficient production in the coculture with OP9 stromal cells and analysis of lymphohematopoietic potential. Blood 105, 617 626.

Wang, Y., Yates, F., Naveiras, O., Ernst, P., Daley, G.Q., 2005. Embryonic stem cell-derived hematopoietic stem cells. Proc. Natl. Acad. Sci. U. S. A. 102, 19081–19086.

Williams, D., Baum, C., 2004. Gene therapy needs both trials and new strategies. Nature 429, 129.

Zhang, X.B., Beard, B.C., Trobridge, G.D., Wood, B.L., Sale, G.E., Sud, R., Humphries, R.K., Kiem, H.P., 2008. High incidence of leukemia in large animals after stem cell gene therapy with a HOXB4-expressing retroviral vector. J. Clin. Invest. 118, 1502–1510.

Efficient Generation of Functional Hepatocytes From Human Embryonic Stem Cells and Induced Pluripotent Stem Cells by HNF4α Transduction

Kazuo Takayama[1,2], Mitsuru Inamura[1,2], Kenji Kawabata[2,3], Kazufumi Katayama[1], Maiko Higuchi[2], Katsuhisa Tashiro[2], Aki Nonaka[2], Fuminori Sakurai[1], Takao Hayakawa[4,5], Miho Kusuda Furue[6,7] and Hiroyuki Mizuguchi[1,2,8]

[1]Laboratory of Biochemistry and Molecular Biology, Graduate School of Pharmaceutical Sciences, Osaka University, Osaka, Japan; [2]Laboratory of Stem Cell Regulation, National Institute of Biomedical Innovation, Osaka, Japan; [3]Laboratory of Biomedical Innovation, Graduate School of Pharmaceutical Sciences, Osaka University, Osaka, Japan; [4]Pharmaceutics and Medical Devices Agency, Tokyo, Japan; [5]Pharmaceutical Research and Technology Institute, Kinki University, Osaka, Japan; [6]JCRB Cell Bank, Division of Bioresources, National Institute of Biomedical Innovation, Osaka, Japan; [7]Laboratory of Cell Processing, Institute for Frontier Medical Sciences, Kyoto University, Kyoto, Japan; [8]The Center for Advanced Medical Engineering and Informatics, Osaka University, Osaka, Japan

Hepatocyte-like cells from human embryonic stem cells (ESCs) and induced pluripotent stem cells (iPSCs) are expected to be a useful source of cells drug discovery. Although we recently reported that hepatic commitment is promoted by transduction of SOX17 and HEX into human ESC- and iPSC-derived cells, these hepatocyte-like cells were not sufficiently mature for drug screening. To promote hepatic maturation, we utilized transduction of the hepatocyte nuclear factor 4α (HNF4α) gene, which is known as a master regulator of liver-specific gene expression. Adenovirus vector-mediated overexpression of HNF4α in hepatoblasts induced by SOX17 and HEX transduction led to upregulation of epithelial and mature hepatic markers such as cytochrome P450 (CYP) enzymes, and promoted hepatic maturation by activating the mesenchymal-to-epithelial transition (MET). Thus HNF4α might play an important role in the hepatic differentiation from human ESC-derived hepatoblasts by activating the MET. Furthermore, the hepatocyte like-cells could catalyze the toxication of several compounds. Our method would be a valuable tool for the efficient generation of functional hepatocytes derived from human ESCs and iPSCs, and the hepatocyte-like cells could be used for predicting drug toxicity.

Received 19 July 2011; accepted 28 September 2011; published online 8 November 2011. doi:10.1038/mt.2011.234

INTRODUCTION

Human embryonic stem cells (ESCs) and induced pluripotent stem cells (iPSCs) are able to replicate indefinitely and differentiate into most of the body's cell types.[1,2] They could provide an unlimited source of cells for various applications. Hepatocyte-like cells, which are differentiated from human ESCs and iPSCs, would be useful for basic research, regenerative medicine, and drug discovery.[3] In particular, it is expected that hepatocyte-like cells will be utilized as a tool for cytotoxicity screening in the early phase of pharmaceutical development. To catalyze the toxication of several compounds, hepatocyte-like cells need to be mature enough to exhibit hepatic functions, including high activity levels of the cytochrome P450 (CYP) enzymes. Because the present technology for the generation of hepatocyte-like cells from human ESCs and iPSCs, which is expected to be utilized for drug discovery, is not refined enough for this application, it is necessary to improve the efficiency of hepatic differentiation. Although conventional methods such as growth factor-mediated hepatic differentiation are useful to recapitulate liver development, they lead to only a heterogeneous hepatocyte population.[4–6] Recently, we showed that transcription factors are transiently transduced to promote hepatic differentiation in addition to the conventional differentiation method which uses only growth factors.[7] Ectopic expression of Sry-related HMG box 17 (SOX17) or hematopoietically expressed homeobox (HEX) by adenovirus (Ad) vectors in human ESC-derived mesendoderm or definitive endoderm (DE) cells markedly enhances the endoderm differentiation or hepatic commitment, respectively.[7,8] However, further hepatic maturation is required for drug screening.

The transcription factor hepatocyte nuclear factor 4α (HNF4α) is initially expressed in the developing hepatic diverticulum on E8.75,[9,10] and its expression is elevated as the liver develops. A previous loss-of-function study showed that HNF4α plays a critical role in liver development; conditional deletion of *HNF4α* in fetal hepatocytes results in the faint expression of many mature hepatic enzymes and the impairment of normal liver morphology.[11] The genome-scale chromatin immunoprecipitation assay showed that HNF4α binds to the promoters of nearly half of the genes expressed in the mouse liver,[12] including cell adhesion and junctional proteins,[13] which are important in the hepatocyte epithelial structure.[14] In addition, HNF4α plays a critical role in hepatic differentiation and in a wide variety of liver functions, including lipid and glucose metabolism.[15,16] Although HNF4α could promote transdifferentiation into hepatic lineage from hematopoietic cells,[17] the function of HNF4α in hepatic differentiation from human ESCs and iPSCs remains unknown. A previous study showed that hepatic differentiation from mouse hepatic progenitor cells is promoted by HNF4α, although many of the hepatic markers that they examined were target genes of HNF4α.[18] They transplanted the HNF4α-overexpressed mouse hepatic progenitor cells to promote hepatic differentiation, but they did not examine the markers that relate to hepatic maturation such as CYP enzymes, conjugating enzymes, and hepatic transporters.

In this study, we examined the role of HNF4α in hepatic differentiation from human ESCs and iPSCs. The human ESC- and iPSC-derived hepatoblasts, which were efficiently generated by sequential transduction of SOX17 and HEX, were transduced with HNF4α-expressing Ad vector (Ad-HNF4α), and then the expression of hepatic markers of the hepatocyte-like cells were assessed. In addition, we examined whether or not the hepatocyte-like cells, which were generated by sequential transduction of SOX17, HEX, and HNF4α, were able to predict the toxicity of several compounds.

RESULTS

Stage-specific HNF4α transduction in hepatoblasts selectively promotes hepatic differentiation

The transcription factor HNF4α plays an important role in both liver generation[11] and hepatic differentiation from human ESCs and iPSCs (**Supplementary Figure S1**). We expected that hepatic differentiation could be accelerated by HNF4α transduction. To examine the effect of forced expression of HNF4α in the hepatic differentiation from human ESC- and iPSC-derived cells, we used a fiber-modified Ad vector.[19] Initially, we optimized the time period for Ad-HNF4α transduction. Human ESC (H9)-derived DE cells (day 6) (**Supplementary Figures S2** and **S3a**), hepatoblasts (day 9) (**Supplementary Figures S2** and **S3b**), or a heterogeneous population consisting of hepatoblasts, hepatocytes, and cholangiocytes (day 12) (**Supplementary Figures S2** and **S3c**) were transduced with Ad-HNF4α and then the Ad-HNF4α-transduced cells were cultured until day 20 of differentiation (**Figure 1**). We ascertained the expression of exogenous *HNF4α* in human ESC-derived hepatoblasts (day 9) transduced with Ad-HNF4α (**Supplementary Figure S4**). The transduction of Ad-HNF4α into human ESC-derived hepatoblasts (day 9) led to the highest expression levels of the hepatocyte markers *albumin* (*ALB*)[20] and *α-1-antitrypsin* (**Figure 1a**). In contrast, the expression levels of the cholangiocyte markers *cytokeratin 7* (*CK7*)[21] and *SOX9*[22] were

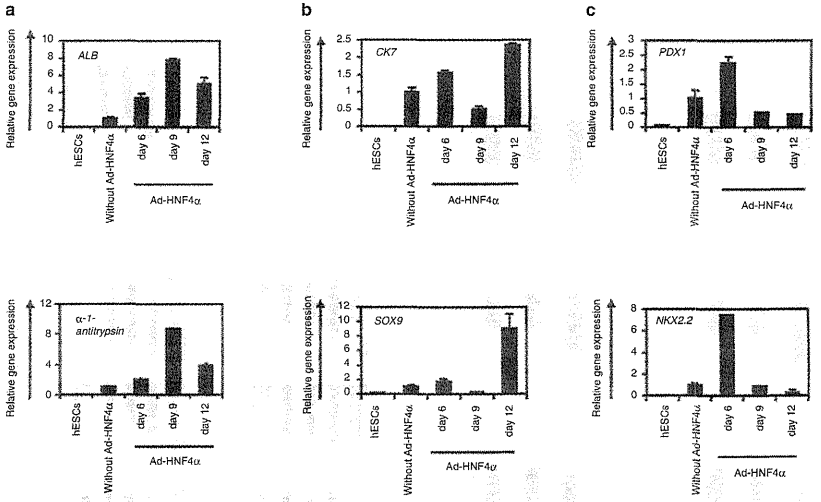

Figure 1 Transduction of HNF4α into hepatoblasts promotes hepatic differentiation. (**a–c**) The human ESC (H9)-derived cells, which were cultured for 6, 9, or 12 days according to the protocol described in **Figure 2a**, were transduced with 3,000 vector particles (VP)/cell of Ad-HNF4α for 1.5 hours and cultured until day 20. The gene expression levels of (**a**) hepatocyte markers (*ALB* and *α-1-antitrypsin*), (**b**) cholangiocyte markers (*CK7* and *SOX9*), and (**c**) pancreas markers (*PDX1* and *NKX2.2*) were examined by real-time RT-PCR on day 0 (human ESCs (hESCs)) or day 20 of differentiation. The horizontal axis represents the days when the cells were transduced with Ad-HNF4α. On the y-axis, the level of the cells without Ad-HNF4α transduction on day 20 was taken as 1.0. All data are represented as means ± SD ($n = 3$). ESC, embryonic stem cell; HNF4α, hepatocyte nuclear factor 4α; RT-PCR, reverse transcription-PCR.

Correspondence: Hiroyuki Mizuguchi, Laboratory of Biochemistry and Molecular Biology, Graduate School of Pharmaceutical Sciences, Osaka University, 1-6 Yamadaoka, Suita, Osaka 565-0871, Japan. E-mail: mizuguch@phs.osaka-u.ac.jp

downregulated in the cells transduced on day 9 as compared with nontransduced cells (**Figure 1b**). This might be because hepatic differentiation was selectively promoted and biliary differentiation was repressed by the transduction of HNF4α in hepatoblasts. The expression levels of the pancreas markers *PDX1*[23] and *NKX2.2*[24] did not make any change in the cells transduced on day 9 as compared with nontransduced cells (**Figure 1c**). Interestingly, the expression levels of the pancreas markers were upregulated, when Ad-HNF4α transduction was performed into DE cells (day 6) (**Figure 1c**). These results suggest that HNF4α might promote not only hepatic differentiation but also pancreatic differentiation, although the optimal stage of HNF4 transduction for the differentiation of each cell is different. We have confirmed that there was no difference between nontransduced cells and Ad-LacZ-transduced cells in the gene expression levels of all the markers investigated in **Figure 1a–c** (data not shown). We also confirmed that Ad vector-mediated gene expression in the human ESC-derived hepatoblasts (day 9) continued until day 14 and almost disappeared on day 18 (**Supplementary Figure S5**). These results indicated that the stage-specific HNF4α overexpression in human ESC-derived hepatoblasts (day 9) was essential for promoting efficient hepatic differentiation.

Transduction of HNF4α into human ESC- and iPSC-derived hepatoblasts efficiently promotes hepatic maturation

From the results of Figure 1, we decided to transduce hepatoblasts (day 9) with Ad-HNF4α. To determine whether hepatic maturation is promoted by Ad-HNF4α transduction, Ad-HNF4α-transduced cells were cultured until day 20 of differentiation according to the schematic protocol described in Figure 2a. After the hepatic maturation, the morphology of human ESCs was gradually changed into that of hepatocytes: polygonal with distinct round nuclei (day 20) (Figure 2b). Interestingly, a portion of the hepatocyte-like cells, which were ALB[20]-, CK18[21]-, CYP2D6-, and CYP3A4[25]-positive cells, had double nuclei, which was also observed in primary human hepatocytes (Figure 2b,c, and **Supplementary Figure S6**). We also examined the hepatic gene expression levels on day 20 of differentiation (Figure 3a,b). The gene expression analysis of *CYP1A2*, *CYP2C9*, *CYP2C19*, *CYP2D6*, *CYP3A4*, and *CYP7A1*[25] showed higher expression levels in all of Ad-SOX17-, Ad-HEX-, and Ad-HNF4α-transduced cells (three factors-transduced cells) as compared with those in both Ad-SOX17- and Ad-HEX-transduced cells (two factors-transduced cells) on day 20 (Figure 3a). The gene expression level of NADPH-CYP reductase

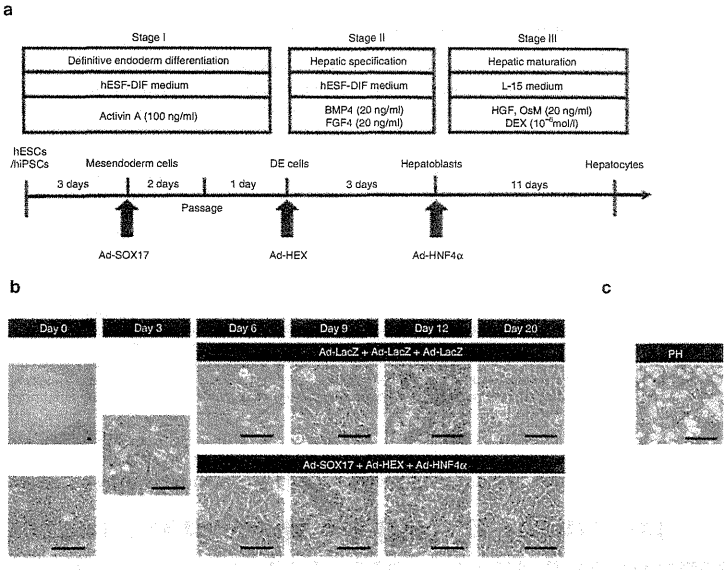

Figure 2 Hepatic differentiation of human ESCs and iPSCs transduced with three factors. (**a**) The procedure for differentiation of human ESCs and iPSCs into hepatocytes via DE cells and hepatoblasts is presented schematically. The hESF-DIF medium was supplemented with 10 μg/ml human recombinant insulin, 5 μg/ml human apotransferrin, 10 μmol/l 2-mercaptoethanol, 10 μmol/l ethanolamine, 10 μmol/l sodium selenite, and 0.5 mg/ml fatty-acid-free BSA. The L15 medium was supplemented with 8.3% tryptose phosphate broth, 8.3% FBS, 10 μmol/l hydrocortisone 21-hemisuccinate, 1 μmol/l insulin, and 25 mmol/l $NaHCO_3$. (**b**) Sequential morphological changes (day 0–20) of human ESCs (H9) differentiated into hepatocytes via DE cells and hepatoblasts are shown. Red arrow shows the cells that have double nuclei. (**c**) The morphology of primary human hepatocytes is shown. Bar represents 50 μm. BSA, bovine serum albumin; DE, definitive endoderm; ESC, embryonic stem cell; iPSC, induced pluripotent stem cell.

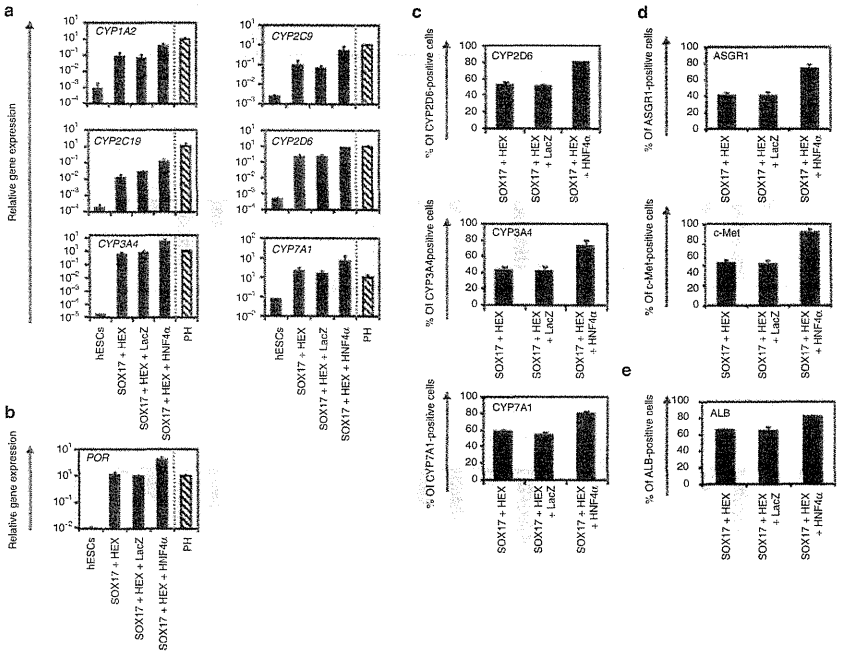

Figure 3 Transduction of HNF4α promotes hepatic maturation from human ESCs and iPSCs. (**a**,**b**) The human ESCs were differentiated into hepatocytes according to the protocol described in **Figure 2a**. On day 20 of differentiation, the gene expression levels of (**a**) CYP enzymes (*CYP1A2*, *CYP2C9*, *CYP2C19*, *CYP2D6*, *CYP3A4*, and *CYP7A1*) and (**b**) *POR* were examined by real-time RT-PCR in undifferentiated human ESCs (hESCs), the hepatocyte-like cells, and primary human hepatocytes (PH, hatched bar). On the y-axis, the expression level of primary human hepatocytes, which were cultured for 48 hours after the cells were plated, was taken as 1.0. (**c–e**) The hepatocyte-like cells (day 20) were subjected to immunostaining with (**c**) anti-drug-metabolizing enzymes (CYP2D6, CYP3A4, and CYP7A1), (**d**) anti-hepatic surface protein (ASGR1 and c-Met), and (**e**) anti-ALB antibodies, and then the percentage of antigen-positive cells was examined by flow cytometry on day 20 of differentiation. All data are represented as means ± SD ($n = 3$). ESC, embryonic stem cell; HNF4α, hepatocyte nuclear factor 4α; iPSC, induced pluripotent stem cell.

(POR)[26], which is required for the normal function of CYPs, was also higher in the three factors-transduced cells (Figure 3b). The gene expression analysis of ALB, α-1-antitrypsin (α-1-AT), transthyretin, hepatic conjugating enzymes, hepatic transporters, and hepatic transcription factors also showed higher expression levels in the three factors-transduced cells (**Supplementary Figures S7** and **S8**). Moreover, the gene expression levels of these hepatic markers of three factor-transduced cells were similar to those of primary human hepatocytes, although the levels depended on the type of gene (Figure 3a,b, and **Supplementary Figures S7** and **S8**). To confirm that similar results could be obtained with human iPSCs, we used three human iPS cell lines (201B7, Dotcom, and Tic). The gene expression of hepatic markers in human ESC- and iPSC-derived hepatocytes were analyzed by real-time reverse transcription-PCR on day 20 of differentiation. Three human iPS cell lines as well as human ESCs also effectively differentiated into hepatocytes in response to transduction of the three factors (**Supplementary Figure S9**). Interestingly, we observed differences in the hepatic maturation efficiency among the three human iPS cell lines. That is, two of the human iPS cell lines (Tic and Dotcom) were more committed to the hepatic lineage than another human iPS cell line (201B7). Because almost homogeneous hepatocyte-like cells would be more useful in basic research, regenerative medicine, and drug discovery, we also examined whether our novel methods for hepatic maturation could generate a homogeneous hepatocyte population by flow cytometry analysis (**Figure 3c–e**). The percentages of CYP2D6-, CYP3A4-, and CYP7A1-positive cells were ~80% in the three factors-transduced cells, while they were ~50% in the two factors-transduced cells (**Figure 3c**). The percentages of hepatic surface antigen (asialoglycoprotein receptor 1 (ASGR1] and met proto-oncogene (c-Met))-positive cells (**Figure 3d**) and ALB-positive cells (**Figure 3e**) were also ~80% in the three factors-transduced cells. These results indicated that a nearly homogeneous population was obtained by our differentiation protocol

using the transduction of three functional genes (SOX17, HEX, and HNF4α).

The three factors-transduced cells have characteristics of functional hepatocytes

The hepatic functions of the hepatocyte-like cells, such as the uptake of low-density lipoprotein (LDL) and CYP enzymes activity, of the hepatocyte-like cells were examined on day 20 of differentiation. Approximately 87% of the three factors-transduced cells uptook LDL in the medium, whereas only 44% of the two factors-transduced cells did so (**Figure 4a**). The activities of CYP enzymes of the hepatocyte-like cells were measured according to the metabolism of the CYP3A4, CYP2C9, or CYP1A2 substrates (Figure 4b). The metabolites were detected in the three factors-transduced cells and their activities were higher than those of the two factors-transduced cells (dimethyl sulfoxide (DMSO) column). We further tested the induction of CYP3A4, CYP2C9, and CYP1A2 by chemical stimulation, since CYP3A4, CYP2C9, and CYP1A2 are the important prevalent CYP isozymes in the liver and are involved in the metabolism of a significant proportion of the currently available commercial drugs (rifampicin or omeprazole column). It is well known that CYP3A4 and CYP2C9 can be induced by rifampicin, whereas CYP1A2 can be induced by omeprazole. The hepatocyte-like cells were treated with either of these. Although undifferentiated human ESCs responsed to neither rifampicin nor omeprazole (data not shown), the hepatocyte-like cells produced more metabolites in response to chemical stimulation as well as primary hepatocytes (**Figure 4b**). The activity levels of the hepatocyte-like cells as compared with those of primary human hepatocytes depended on the types of CYP; the CYP3A4 activity of the hepatocyte-like cells was similar to that of primary human hepatocytes, whereas the CYP2C9 and CYP1A2 activities of the hepatocyte-like cells were slightly lower than those of primary human hepatocytes (**Figure 3a**). These results indicated that high levels of functional CYP enzymes were detectable in the hepatocyte-like cells.

The metabolism of diverse compounds involving uptake, conjugation, and the subsequent release of the compounds is an important function of hepatocytes. Uptake and release of Indocyanine green (ICG) can often be used to identify hepatocytes in ESC differentiation models.[27] To investigate this function in our hepatocyte-like cells, we compared this ability of the three factors-transduced cells with that of the two factors-transduced cells on day 20 of differentiation (**Figure 4c**). The three factors-transduced cells had more ability to uptake ICG and to excrete ICG by culturing without ICG for 6 hours. We also examined whether the hepatocyte-like cells could store glycogen, a characteristic of functional hepatocytes (**Figure 4d**). On day 20 of differentiation, the three factors-transduced cells and the two factors-transduced cells were stained for cytoplasmic glycogen using the Periodic Acid-Schiff staining procedure. The three factors-transduced cells exhibited more abundant storage of glycogen than the two-factors-transduced cells. These results showed that abundant hepatic functions, such as uptake and excretion of ICG and storage of glycogen, were obtained by the transduction of three factors.

Many adverse drug reactions are caused by the CYP-dependent activation of drugs into reactive metabolites.[28] In order to examine metabolism-mediated toxicity and to improve the safety of drug candidates, primary human hepatocytes are widely used.[28] Because primary human hepatocytes have quite different characteristics among distinct lots and because it is difficult to purchase large amounts of primary human hepatocytes that have the same characteristics, hepatocyte-like cells are expected to be used for this purpose. To examine whether our hepatocyte-like cells could be used to predict metabolism-mediated toxicity, the hepatocyte-like cells were incubated with four substrates (troglitazone, acetaminophen, cyclophosphamide, and carbamazepine), which are known to generate toxic metabolites by CYP enzymes, and then the cell viability was measured (Figure 4e). The cell viability of the two factors plus Ad-LacZ-tansduced cells were higher than that of the three factors-transduced cells at each different concentration of four test compounds. These results indicated that the three factors-transduced cells could more efficiently metabolize the test compounds and thereby induce higher toxicity than either the two factors-transduced cells or undifferentiated human ESCs. The cell viability of the three factors-transduced cells was slightly higher than that of primary human hepatocytes.

HNF4α promotes hepatic maturation by activating mesenchymal-to-epithelial transition

HNF4α is known as a dominant regulator of the epithelial phenotype because its ectopic expression in fibroblasts (such as NIH 3T3 cells) induces mesenchymal-to-epithelial transition (MET)[11], although it is not known whether HNF4α can promote MET in hepatic differentiation. Therefore, we examined whether HNF4α transduction promotes hepatic maturation from hepatoblasts by activating MET. To clarify whether MET is activated by HNF4α transduction, the human ESC-derived hepatoblasts (day 9) were transduced with Ad-LacZ or Ad-HNF4α, and the resulting phenotype was analyzed on day 12 of differentiation (Figure 5). This time, we confirmed that HNF4α transduction decreased the population of N-cadherin (hepatoblast marker)-positive cells,[29] whereas it increased that of ALB (hepatocyte marker)-positive cells (**Figure 5a**). The number of CK7 (cholangiocyte marker)-positive population did not change (Figure 5a). To investigate whether these results were attributable to MET, the alteration of the expression of several mesenchymal and epithelial markers was examined (**Figure 5b**). The human ESC-derived hepatoblasts (day 9) were almost homogeneously N-cadherin[30] (mesenchymal marker)-positive and E-cadherin[11] (epithelial marker)-negative, demonstrating that human ESC-derived hepatoblasts have mesenchymal characteristics (Figure 5a,b). After HNF4α transduction, the number of E-cadherin-positive cells was increased and reached ~90% on day 20, whereas that of N-cadherin-positive cells was decreased and was less than 5% on day 20 (**Supplementary Figure S10**). These results indicated that MET was promoted by HNF4α transduction in hepatic differentiation from hepatoblasts. Interestingly, the number of growing cells was decreased by HNF4α transduction (**Figure 5c**), and the cell growth was delayed by HNF4α transduction (**Supplementary Figure S11**). This decrease in the number of growing cells might have been because the differentiation was promoted by HNF4α transduction. We also confirmed that MET was promoted by HNF4α transduction in the gene expression levels (Figure 5d).

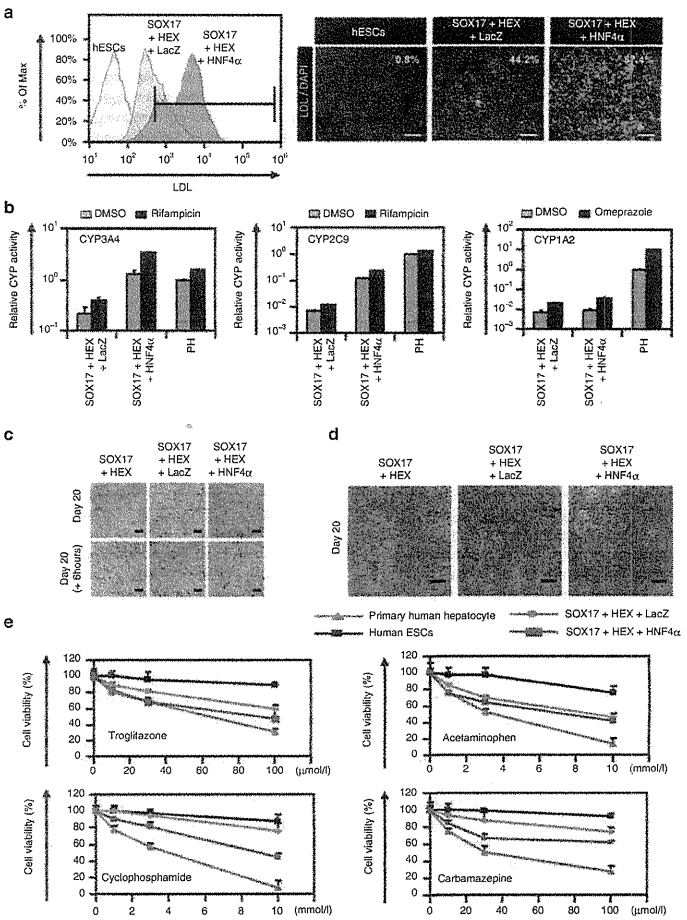

Figure 4 Transduction of the three factors enhances hepatic functions. The human ESCs were differentiated into hepatoblasts and transduced with 3,000 VP/cell of Ad-LacZ or Ad-HNF4α for 1.5 hours and cultured until day 20 of differentiation according to the protocol described in **Figure 2a**. The hepatic functions of the two factors plus Ad-LacZ-transduced cells (SOX17+HEX+LacZ) and the three factors-transduced cells (SOX17+HEX+HNF4α) were compared. (**a**) Undifferentiated human ESCs (hESCs) and the hepatocyte-like cells (day 20) were cultured with medium containing Alexa-Flour 488-labeled LDL (green) for 1 hour, and immunohistochemistry and flow cytometry analysis were performed. The percentage of LDL-positive cells was measured by flow cytometry. Nuclei were counterstained with DAPI (blue). The bar represents 100 μm. (**b**) Induction of CYP3A4 (left), CYP2C9 (middle), or CYP1A2 (right) by DMSO (gray bar), rifampicin (black bar), or omeprazole (black bar) in the hepatocyte-like cells (day 20) and primary human hepatocytes (PH), which were cultured for 48 hours after the cells were plated. On the y-axis, the activity of primary human hepatocytes that have been cultured with medium containing DMSO was taken as 1.0. (**c**) The hepatocyte-like cells (day 20) (upper column) were examined for their ability to take up Indocyanin Green (ICG) and release it 6 hours thereafter (lower column). (**d**) Glycogen storage of the hepatocyte-like cells (day 20) was assessed by Periodic Acid-Schiff (PAS) staining. PAS staining was performed on day 20 of differentiation. Glycogen storage is indicated by pink or dark red-purple cytoplasms. The bar represents 100 μm. (**e**) The cell viability of undifferentiated human ESCs (black), two factors plus Ad-LacZ-tansduced cells (green), the three factors-transduced cells (blue), and primary human hepatocytes (red) was assessed by Alamar Blue assay after 48 hours exposure to different concentrations of four test compounds (troglitazone, acetaminophen, cyclophosphamide, and carbamazepine). The cell viability is expressed as a percentage of cells treated with solvent only treat: 0.1% DMSO except for carbamazepine: 0.5% DMSO. All data are represented as means ± SD (n = 3). ESC, embryonic stem cell; DMSO, dimethyl sulfoxide; LDL, low-density lipoprotein.